Definition of the Spatial Propagator and Implications for Magnetic Field Properties

Justin K. Edmondson[1] · **Pascal Démoulin[2]**

Abstract We present a theoretical framework to analyze the 3D coronal vector magnetic field structure. We assume the vector magnetic field exists and is *a-priori* smooth. We introduce a generalized field line connectivity phase space associated to the vector magnetic field in which the basic elements are the *field line* and its linearized variation, the *spatial propagator*. We provide a direct formulation of these elements in terms of the vector magnetic field and its spatial derivatives, constructed with respect to general curvilinear coordinates and the equivalence class of general affine parameterizations. The spatial propagator describes the geometric organization of the local bundle of field lines, equivalent to kinematic deformation of a propagated volume tied to the bundle. The spatial propagator properties are characterized by dilation, anisotropic stretch, and rotation. Extreme singular values of the spatial propagator describe QSLs, while true separatrix surfaces, respectively separator lines, are identified in the limiting cases of one, respectively two, zero singular values. Finally, we show that, among other possible applications, the Q-factor is easily constructed from analysis of particular sub-matrices of the spatial propagator.

Keywords: Magnetic fields, Corona; Corona, Structures

1. Introduction

Geometry describes the measurable lengths and angles associated with a system's configuration, whereas topology is concerned with those properties preserved

✉ J.K. Edmondson
jkedmond@umich.edu

✉ P. Démoulin
pascal.demoulin@obspm.fr

[1]   Department of Climate and Space Science and Engineering, University of Michigan, 2455 Hayward St., Ann Arbor, MI 48109, USA

[2]   LESIA, Observatoire de Paris, Université PSL, CNRS, Sorbonne Université, Univ. Paris Diderot, Sorbonne Paris Cite, 5 place Jules Janssen, 92195 Meudon, France

under continuous deformation. Over the past several decades the importance of the geometric and topological features to fluid and plasma dynamics has become increasingly clear (see e.g., Moffatt et al., 1991; Arnold & Khesin, 1992; Ricca, 2001). Algebraic and geometric analysis of magnetic and hydrodynamic structures have provided significant development in the context of general plasma equilibria (e.g., Moffatt, 1985, 1986), stability (e.g., Bulanov & Sasorov, 1978; Syrovatskii, 1981; Bulanov et al., 1999), reconnection (Hesse & Schindler, 1988; Schindler et al., 1988; Ruzmaikin & Akhmetiev, 1994; Bulanov et al., 2002; Pontin et al., 2005), heating and wave generation (Ruzmaikin & Berger, 1998). In particular, geometric and topological analyses of the solar coronal magnetic fields have focused on understanding the heating and dynamics (Antiochos, 1987; Berger, 1994; Priest et al., 2005), as well as investigations into the eruptive phenomenology of flares (Mandrini et al., 1995; Démoulin et al., 1997; Titov & Démoulin, 1999; Aulanier et al., 2000) and coronal mass ejection (CME) initiation (Antiochos et al., 1999; Lynch et al., 2008; Lynch & Edmondson, 2013).

The build-up, storage, transport, and subsequent release of magnetic energy in the low-beta solar corona is widely accepted as the basic requirement for solar coronal heating, the origin and generation of the solar wind, as well as eruptive phenomenology and space weather prediction (see e.g., Klimchuk, 2006, for review). Such dynamics in the low-beta coronal plasma environment are governed by the geometric and topological features of coronal magnetic field (see Longcope, 2005, for review). In general, non-trivial geometric and topological features such as null point structure (Lau & Finn, 1990; Parnell et al., 1996), separator lines (Longcope & Cowley, 1996), bald patches (Seehafer, 1986; Wolfson, 1989; Low, 1992; Titov et al., 1993), separatrix surfaces (Low, 1987; Somov, 1992; Priest et al., 2002) and quasi-separatrix layers (QSLs; Priest & Démoulin, 1995; Démoulin et al., 1996, 1997; Titov, 1999; Milano et al., 1999) appear ubiquitously in the coronal magnetic field. In fact, the current state of global solar wind generation models (see e.g., Abbo et al., 2016, for recent review), differ to the extent and complexity of these geometric and topological structures within the coronal magnetic field (e.g., Wang & Sheeley, 1990; Fisk et al., 1998; Arge & Pizzo, 2000; Fisk, 2003; Cranmer et al., 2007; Antiochos et al., 2011; Antiochos, 2013).

Since the vector magnetic field is reference frame dependent, so too is the magnetic connectivity description (Hornig & Schindler, 1996); in fact, the entire concept of a magnetic field line is not Lorentz invariant (Hornig, 1997). However, in a fixed reference frame, the geometric and topological features of the magnetic field constrain the dynamics. In general, the geometric features and topological constraints of the magnetic field are primarily important to understand where and how energy is stored and released in low-beta plasma environments such as the solar corona. In the presence of resistive (non-ideal) physics, field line connectivity topology is no longer preserved, though separatrix structures remain. Separatrix surfaces and QSLs are associated with electric current sheet formation and reconnection, and therefore it is the geometry of these structures that constrain the storage of magnetic energy throughout the coronal volume, and determine both the location and the ability to release free-energy (see references above). In particular, QSL locations are related to observations of sudden

flare brightening in Hα for a wide variety of solar flare phenomenology such as circular ribbon flares, two ribbon flares, and twisted flux rope (sigmoidal active region) morphologies (see e.g., Janvier, 2017, and references therein). Furthermore, separatrix surfaces and QSLs are the boundaries dividing regions of disparate connectivity in complex, multi-polar coronal structures. Hence, QSLs feature prominently in the rapid reorganization of the vector magnetic field and subsequent energy release in CME initiation mechanisms (see e.g., Aulanier et al., 2005; Effenberger et al., 2011; Janvier et al., 2014; Schmieder et al., 2015; Lynch et al., 2016, and reference therein).

The features of magnetic connectivity map such as helicity, separatrix and QSL structures, and their effect on the system dynamics find their most explicit representations in terms of the algebraic and geometric descriptions of the field line and the field line bundle. In other words, the constraints on the system dynamics become transparent when cast in terms of the geometric structure and topological invariants of field line bundle and its behavior. Numerical magnetohydrodynamic (MHD) methodologies allow one to explore the locus of system dynamics for various magnetic field models, thermodynamic heating models, and boundary conditions. While the MHD method (where applicable) is correct, the MHD equations and numerical solutions are often opaque to these explicit geometric structures (e.g., QSLs, separatrices, and separators) and their behavior. Moreover, many numerical difference schemes are based on linear interpolation which can be a fundamental limitation of the code as an accurate representation of the magnetic field structure, simply shifting the problem of investigating small scale dynamics from physical quantities, such as the vector magnetic field, to finer and more complex numerical grid resolutions. This is an extremely popular approach to numerical/computational solar, and space plasma physics, which arguably leads to spurious physics; we offer no judgement regarding the veracity of these approaches. This perspective, however, requires the development of new mathematical tools/description/framework to analyze the geometric organization of the magnetic field connectivity map.

The purpose of this manuscript is the introduction, development, and presentation of a generalized phase space of field line geometry associated to the vector magnetic field, in which the geometric structure and topological constraints are made explicit. This formalism does not alter the physics of Maxwell's equations, or MHD, but is a fundamentally different framework which describes and analyzes vector magnetic fields. The basic assumptions of this framework are:

1. the vector magnetic field is the *primary (observable)* quantity that satisfies some standard physical evolutions (e.g., Maxwell's equations, MHD induction, etc.), and the connectivity map is the *secondary (derived)* quantity; and
2. while large gradients may exist, the vector magnetic field is *a-priori* smooth everywhere at the smallest scales.

Under these assumptions, we derive a generally covariant measure of the local field geometry, called the *Spatial Propagator*, from the linearized variation of a field line. We demonstrate that the spatial propagator characterizes the geometric organization of a local bundle of field lines. Moreover, we identify topological invariants derived from the spatial propagator, as well as demonstrate the proper

limiting connection to QSLs, separatrix surfaces, and separator lines. Beyond the limiting cases, the inclusion and analysis of existing and/or generated singular structures within the vector field are outside the scope of the present work.

The roadmap for this paper is as follows. In Section 2 we lay out a precise mathematical definition for the field lines of a vector field (Section 2.1). We introduce the Spatial Propagator (Section 2.2) as a generalized spatial variation of an entire field line solution, which describes the local bundle of field lines. Furthermore, we derive a direct relation between the spatial propagator and the local gradient of the vector field (Section 2.3), and hence, the precise mathematical formulation of the geometric phase space, consisting of the integral curve solutions and their associated spatial propagators. Finally, we discuss the various representations of the spatial propagator (Section 2.4): covariance with respect to local curvilinear coordinates, and equivalence with respect to affine transformations of the coordinate defined along the field line.

In Section 3 we characterize the geometric organization (dilation, rotation, anisotropic stretch, and connectivity gradient) of a local bundle of field lines using a mathematically equivalent kinematic analysis of a volume propagated and deformed by the bundle. We explore the vector field geometry using the spatial propagator in terms of volumetric dilation (Section 3.1), from which we identify a topological invariant measure that reflects the divergence-free condition of physical magnetic fields. We demonstrate that the singular values and singular vectors of the spatial propagator characterize the anisotropic stretch and rigid-body rotation deformations of the geometry (Section 3.2). Lastly (Section 3.3), we demonstrate the construction of the Q-factor (see e.g., Titov et al., 2002; Titov, 2007) by a simple example, and hence directly identify quasi-separatrix structures directly from the spatial propagator.

We close with a description of other potential applications of the Spatial Propagator in Section 4. The major objects and main equations of this framework are summarized in Table 1.

2. The Integral Curve Description of Vector Field Geometry

Let $M \subseteq \mathbb{R}^3$ be a subset of three dimensional space, possibly with boundary ∂M. Let $\boldsymbol{B}(\boldsymbol{r})$ be a time-dependent vector field for all positions $\boldsymbol{r} \in M$ and times $t \in \mathbb{R}$. This field satisfies some set of dynamic evolution equations for some known initial and boundary conditions. Written with respect to a Cartesian[1] basis $\{\boldsymbol{e}_x, \boldsymbol{e}_y, \boldsymbol{e}_z\}$, the vector field $\boldsymbol{B}(\boldsymbol{r})$ has component functions,

$$
\begin{aligned}
\boldsymbol{B}(\boldsymbol{r}) \cdot \boldsymbol{e}_x &= (\left.\boldsymbol{B}\right|_{\boldsymbol{r}})^x = B^x(x, y, z, t), \\
\boldsymbol{B}(\boldsymbol{r}) \cdot \boldsymbol{e}_y &= (\left.\boldsymbol{B}\right|_{\boldsymbol{r}})^y = B^y(x, y, z, t), \\
\boldsymbol{B}(\boldsymbol{r}) \cdot \boldsymbol{e}_z &= (\left.\boldsymbol{B}\right|_{\boldsymbol{r}})^z = B^z(x, y, z, t),
\end{aligned}
\tag{1}
$$

---

[1]We remark, unless specifically noted otherwise, throughout this paper we work with respect to the standard Cartesian coordinates $\{x, y, z\}$ and orthonormal Cartesian unit basis vectors $\{\boldsymbol{e}_x, \boldsymbol{e}_y, \boldsymbol{e}_z\}$.

Table 1. A summary of quantities.

Symbol	Quantity Name	Equations	Section
$\boldsymbol{B}\left(\boldsymbol{r}\right)$	Vector field	(2)	§2.1
λ	Connectivity parameter	(2)	§2.1
$\boldsymbol{r}_0$	Reference point	(3)	§2.1
$\boldsymbol{r}\left(\lambda,\boldsymbol{r}_0\right)$	Field line (for single fixed $\boldsymbol{r}_0$)	(2)	§2.1
$\boldsymbol{r}\left(\lambda,\boldsymbol{r}_0\right)$	Congruence (for all $\boldsymbol{r}_0 \in \Omega_0 \subset \mathbb{R}^3$)	(2)	§2.1
$\nabla\boldsymbol{B}\left(\boldsymbol{r}\right)$	Covariant differential vector field matrix	(15)	§2.2
$\mathbf{F}\left(\lambda,\boldsymbol{r}_0\right)$	Spatial Propagator	(11), (16)	§2.2
$\boldsymbol{v}\left(\lambda,\boldsymbol{r}_0\right)$	Propagated shift vector	(12)	§2.2
$\boldsymbol{h} = \boldsymbol{v}\left(0,\boldsymbol{r}_0\right)$	Reference shift vector	(10), (12)	§2.2
$\mathrm{d}\Omega\left(\lambda,\boldsymbol{r}_0\right)$	Signed differential volume element	(29)	§3.1
$\Omega\left(\lambda,\boldsymbol{r}_0\right)$	Total propagated volume	(31)	§3.1
$\sigma_\alpha\left(\lambda,\boldsymbol{r}_0\right)$	Singular values of $\mathbf{F}\left(\lambda,\boldsymbol{r}_0\right)$	(37)	§3.2
$\hat{\boldsymbol{l}}_\alpha\left(\lambda,\boldsymbol{r}_0\right),\hat{\boldsymbol{r}}_\alpha\left(\lambda,\boldsymbol{r}_0\right)$	Left-, Right-Singular vectors of $\mathbf{F}\left(\lambda,\boldsymbol{r}_0\right)$	(42)	§3.2
$\mathbf{V}\left(\lambda,\boldsymbol{r}_0\right),\mathbf{U}\left(\lambda,\boldsymbol{r}_0\right)$	Left-, Right-Stretch matrices	(40), (46)	§3.2
$\mathbf{R}\left(\lambda,\boldsymbol{r}_0\right)$	Rotation matrix	(41), (46)	§3.2
$Q\left(\lambda,\boldsymbol{r}_0\right)$	Squashing factor (Q-Value)	(56), (60)	§3.3

where $\boldsymbol{r}$ and t are, respectively, the spatial position and time.

In general, the vector field $\boldsymbol{B}\left(\boldsymbol{r}\right)$ is time-dependent, and therefore, strictly speaking, so too are the integral curves (Section 2.1), the spatial propagator (Section 2.2), as well as all other objects constructed therefrom. For ease of notation, throughout this work we suppress the functional time-dependence of all quantities; this may be interpreted as analyzing the system at a fixed time, or for very-low frequency dynamics, $f \ll c/L$ where c is the characteristic speed of communication, and L a characteristic length scale. The dynamical description of the integral curves (Section 2.1), the spatial propagator (Section 2.2), etc. require a treatment of the full four-dimensional electromagnetic field tensor (Jackson, 1999, §11.9), which is outside the scope of this work.

2.1. The Integral Curves of a Vector Field

In differential equation theory, a general vector field $\boldsymbol{B}\left(\boldsymbol{r}\right)$ is everywhere tangent to a set of integral curves $\boldsymbol{r}\left(\lambda,\boldsymbol{r}_0\right)$ which satisfy the initial value problem,

$$\frac{\partial\boldsymbol{r}\left(\lambda,\boldsymbol{r}_0\right)}{\partial\lambda} = \boldsymbol{B}\left(\boldsymbol{r}\right), \tag{2}$$

$$\boldsymbol{r}\left(0,\boldsymbol{r}_0\right) = \boldsymbol{r}_0. \tag{3}$$

The family of integral curve solutions $\boldsymbol{r}\left(\lambda,\boldsymbol{r}_0\right)$ are parametrized by a real number $\lambda \in \mathbb{R}$, referred to as the *connectivity parameter*, and a three component vector $\boldsymbol{r}_0 \in M$, referred to as the *reference point*. A single integral curve, as a particular solution to Equations (2) and (3), is identified by a single fixed reference point $\boldsymbol{r}_0$. The connectivity parameter λ denotes the distance per unit field strength along

any particular solution curve issuing from a particular reference point. We note, the rate of change with respect to λ is simply the directional derivative along the vector field, which may be written with respect to the coordinate representation

$$\frac{\partial}{\partial \lambda} := \boldsymbol{B}\left(\boldsymbol{r}\right) \cdot \nabla. \tag{4}$$

The integral curve solutions to Equations (2) and (3) represent position vectors $\boldsymbol{r} = \boldsymbol{r}\left(\lambda, \boldsymbol{r}_0\right)$, the components of which are functions of $\left(\lambda, \boldsymbol{r}_0\right)$; written with respect to a Cartesian basis $\{\boldsymbol{e}_x, \boldsymbol{e}_y, \boldsymbol{e}_z\}$,

$$
\begin{aligned}
\boldsymbol{r}\left(\lambda, \boldsymbol{r}_0\right) \cdot \boldsymbol{e}_x &= \left(\left.\boldsymbol{r}\right|_{\lambda, \boldsymbol{r}_0}\right)^x = x\left(\lambda, x_0, y_0, z_0\right), \\
\boldsymbol{r}\left(\lambda, \boldsymbol{r}_0\right) \cdot \boldsymbol{e}_y &= \left(\left.\boldsymbol{r}\right|_{\lambda, \boldsymbol{r}_0}\right)^y = y\left(\lambda, x_0, y_0, z_0\right), \\
\boldsymbol{r}\left(\lambda, \boldsymbol{r}_0\right) \cdot \boldsymbol{e}_z &= \left(\left.\boldsymbol{r}\right|_{\lambda, \boldsymbol{r}_0}\right)^z = z\left(\lambda, x_0, y_0, z_0\right).
\end{aligned} \tag{5}
$$

The integral curve solutions $\boldsymbol{r}\left(\lambda, \boldsymbol{r}_0\right)$ are known by various names depending on the nature and interpretation of the differential equations and vector field. In physics, integral curves for electric and magnetic fields are known as *field lines*, whereas the integral curves for a velocity field are called *streamlines*. In general dynamical systems theory, the integral curves of the governing differential equation system are referred to as *trajectories* or *orbits*.

Since we find application to solar magnetic fields, throughout this paper we use *field line* to denote a single particular integral curve solution to Equations (2) and (3) for fixed $\boldsymbol{r}_0$. Moreover, a *flux tube* is a *congruence of integral curves* (or simply a *congruence*); that is, a local bundle of field lines defined by a particular set of reference points in some neighborhood $\boldsymbol{r}_0 \in \Omega_0 \subseteq M$ (see Figure 1).
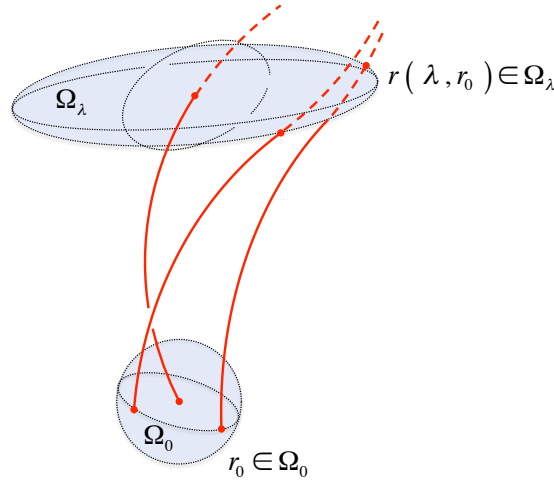
Figure 1. Illustration of a general congruence viz. field lines and reference points. A particular field line $\boldsymbol{r}\left(\lambda, \boldsymbol{r}_0\right)$ is associated with a single fixed reference point $\boldsymbol{r}_0$. A congruence is defined by a set of reference points in some neighborhood $\boldsymbol{r}_0 \in \Omega_0 \subseteq \mathbb{R}^3$.

We make a few observations and define some nomenclature regarding the field lines in physical systems of interest. The $\lambda = 0$ datum defined by the reference

point $\boldsymbol{r}_0 = \boldsymbol{r}\left(0, \boldsymbol{r}_0\right)$ is typically referred to as the *launch foot point* in magnetic systems. A reference point $\boldsymbol{r}_0$ is a free-parameter, typically chosen on the system boundary, or to coincide with some known initial state within the system interior; for example, in a magnetized plasma this choice typically coincides with a highly-conductive parcel of plasma material. The point $\boldsymbol{r} = \boldsymbol{r}\left(L, \boldsymbol{r}_0\right)$ for a *finite* $\lambda = L$, corresponding to the final point of integration of Equations (2) and (3) is often referred to as the *target foot point* in magnetic systems; typically, the target foot points is where the integral curves crosses the system boundary, or encounters a singularity of the vector field. In this paper, unless explicitly stated, we consider a finite connectivity parameter interval $\lambda \in [0, L]$.

The congruence of integral curves of a smooth vector field represents an equivalence class under general affine transformations of the connectivity parameter of the form $\lambda \mapsto \ell\left(\lambda\right) = f\left(\boldsymbol{r}\right)\lambda + b$, where $f\left(\boldsymbol{r}\right)$ is a smooth, positive definite, scalar-valued function[2], and $b \in \mathbb{R}$ an arbitrary constant[3]. The re-parametrized flow $\boldsymbol{r}\left(\ell, \boldsymbol{r}_b\right)$ satisfies Equations (2) and (3) for vector field $\boldsymbol{X}\left(\boldsymbol{r}\right) = \boldsymbol{B}\left(\boldsymbol{r}\right)/f\left(\boldsymbol{r}\right)$ and reference condition $\boldsymbol{r}_b$; that is,

$$\frac{\partial \boldsymbol{r}\left(\ell, \boldsymbol{r}_0\right)}{\partial \ell} = \boldsymbol{X}\left(\boldsymbol{r}\right), \qquad (6)$$

$$\boldsymbol{r}\left(b, \boldsymbol{r}_0\right) = \boldsymbol{r}_b. \qquad (7)$$

A simple application of this $\lambda \mapsto \ell\left(\lambda\right)$ re-parametrization is the analysis of the $\boldsymbol{B}$ field in a system with boundaries ∂M. One has the freedom to choose the function $f\left(\boldsymbol{r}\right)$ (and constant $b = 0$) in order that the values $\ell = 0$ and $\ell = 1$ coincide with the initial and final points of the field lines taken at the boundary surfaces, $\boldsymbol{r}_0 \in \partial M$ and $\boldsymbol{r}\left(1, \boldsymbol{r}_0\right) \in \partial M$; typically at the photosphere for solar coronal applications. With $\ell = 0$ and $\ell = 1$ as boundary values, the connectivity parameter ℓ is not the physical (dimensional) arc length, but rather a normalized dimensionless arc length parameter.

As a second application, consider $f\left(\boldsymbol{r}\right) = |\boldsymbol{B}\left(\boldsymbol{r}\right)|$; assuming $|\boldsymbol{B}\left(\boldsymbol{r}\right)| \neq 0$. The vector field $\boldsymbol{X}\left(\boldsymbol{r}\right) = \dfrac{\boldsymbol{B}\left(\boldsymbol{r}\right)}{|\boldsymbol{B}\left(\boldsymbol{r}\right)|} = \hat{\boldsymbol{b}}\left(\boldsymbol{r}\right)$ is well defined, and is identified with the unit magnetic field direction. For simplicity and without loss of generality, we may set the constant $b = 0$. Under this transformation, the system of Equations (2) and (3) become

$$\frac{\partial \boldsymbol{r}\left(\ell, \boldsymbol{r}_0\right)}{\partial \ell} = \hat{\boldsymbol{b}}\left(\boldsymbol{r}\right), \qquad (8)$$

$$\boldsymbol{r}\left(0, \boldsymbol{r}_0\right) = \boldsymbol{r}_0 \qquad (9)$$

---

[2]The function f must be at least C^1 differentiable. The positivity condition preserves field line orientation. Furthermore, a solenoidal vector field $\nabla \cdot \boldsymbol{B} = 0$ with $\boldsymbol{X} = \boldsymbol{B}/f$ leads to a constraint $\nabla \cdot \boldsymbol{X} + \boldsymbol{X} \cdot \nabla f = 0$; hence, choosing a function f such that the vector field, $\boldsymbol{X}$, is everywhere tangent to the level surfaces of f, that is $\boldsymbol{X} \cdot \nabla f = 0$ preserves the solenoidal property of the vector field $\boldsymbol{X}$. Furthermore, including a time dependence on f imposes a constraint equation on the $\boldsymbol{X}$-evolution to preserve consistency with $\boldsymbol{B}$.

[3]The value of the constant b represents a relabeling of the reference point on the particular field line solution; i.e., $\boldsymbol{r}_0 \mapsto \boldsymbol{r}_b$.

In this example, the connectivity parameter ℓ represents the physical arc length along the magnetic field line. We refer to the representation constructed from the unit magnetic field direction vector field and in which the connectivity parameter represents the physical arc length along the field line issuing from the reference point, as the *arc length representation.*

2.2. The Spatial Propagator: A Local Congruence of Integral Curves

The relative geometry of a local congruence (i.e., dilation, anisotropic stretch, and rotation of the bundle of curves) is completely described by examining a field line under a spatial variation of the reference point $\boldsymbol{r}_0 \mapsto \boldsymbol{r}_0 + \boldsymbol{h}$. We denote the spatial variation of the reference point by the *reference shift vector $\boldsymbol{h}$.*

Recall, a fixed reference point $\boldsymbol{r}_0$ is equivalent to a particular field line $\boldsymbol{r}(\lambda, \boldsymbol{r}_0)$; hence, when considering solutions to Equations (2) and (3), $\boldsymbol{r}(\lambda, \boldsymbol{r}_0)$ for a set of $\boldsymbol{r}_0 \in \Omega_0$, a variation in the reference point $\boldsymbol{r}_0 \rightarrow \boldsymbol{r}_0 + \boldsymbol{h}$ is equivalent to a variation of the *entire* field line. To see this, consider two spatially neighboring field line solutions within the congruence, respectively, $\boldsymbol{r}(\lambda, \boldsymbol{r}_0)$ and $\boldsymbol{r}(\lambda, \boldsymbol{r}_0 + \boldsymbol{h})$. For all λ, we may relate the component functions of the neighboring field lines by Taylor expansion, such that for $|\boldsymbol{h}| << h_m$,

$$(\left. \boldsymbol{r} \right|_{\lambda, \boldsymbol{r}_0 + \boldsymbol{h}})^i - (\left. \boldsymbol{r} \right|_{\lambda, \boldsymbol{r}_0})^i = \sum_j \frac{\partial (\left. \boldsymbol{r} \right|_{\lambda, \boldsymbol{r}_0})^i}{\partial \boldsymbol{r}_0{}^j} \, h^j + O\left(|\boldsymbol{h}|^2\right), \qquad (10)$$

where h_m is a local characteristic scale length defined by comparing the magnitude of the first-order with the higher-order variational terms (see Appendix A).

Equation (10) describes the local organization of all field lines with reference points within an initial volume Ω_0 of characteristic size $|\Omega_0|^{1/3} << h_m$; that is to say, the congruence is *local* with respect to reference points $\boldsymbol{r}_0 + \boldsymbol{h} \in \Omega_0$ with $|\boldsymbol{h}| << h_m$.

We remark, there is an implicit assumption in (10) that the magnetic vector field $\boldsymbol{B}(\boldsymbol{r})$ is described by smooth component functions everywhere within the domain. In future work, we will explore the consequences of relaxing this assumption.

We define this first order variation of the field line $\boldsymbol{r}(\lambda, \boldsymbol{r}_0)$ with respect to a spatial variation in the reference point $\boldsymbol{r}_0$ to be the *spatial propagator* $\mathbf{F}(\lambda, \boldsymbol{r}_0)$. Then for all λ, the variational derivative may be represented as a 3×3 matrix whose component functions are simply the derivatives of Equations (5) with respect to the reference point components,

$$(\left. \mathbf{F} \right|_{\lambda, \boldsymbol{r}_0})^i{}_j := \frac{\partial (\left. \boldsymbol{r} \right|_{\lambda, \boldsymbol{r}_0})^i}{\partial \boldsymbol{r}_0{}^j} = \begin{pmatrix} \dfrac{\partial x}{\partial x_0} & \dfrac{\partial x}{\partial y_0} & \dfrac{\partial x}{\partial z_0} \\[2mm] \dfrac{\partial y}{\partial x_0} & \dfrac{\partial y}{\partial y_0} & \dfrac{\partial y}{\partial z_0} \\[2mm] \dfrac{\partial z}{\partial x_0} & \dfrac{\partial z}{\partial y_0} & \dfrac{\partial z}{\partial z_0} \end{pmatrix}. \qquad (11)$$

Note, at $\lambda = 0$, Equation (10) reduces to the definition of the reference shift vector, $\boldsymbol{r}(0, \boldsymbol{r}_0 + \boldsymbol{h}) - \boldsymbol{r}(0, \boldsymbol{r}_0) = \mathbf{I} \cdot \boldsymbol{h} = \boldsymbol{h}$. Similarly, at $\lambda = 0$, the field line $\boldsymbol{r}(0, \boldsymbol{r}_0) = \boldsymbol{r}_0$ reduces to the reference point, and thus Equation (11) is simply the 3×3 Identity matrix, $(\left.\mathbf{F}\right|_{0, \boldsymbol{r}_0})^i{}_j = \delta^i{}_j$; where $\delta^i{}_j$ is the Kronecker delta.

The spatial propagator $\mathbf{F}(\lambda, \boldsymbol{r}_0)$ may be considered as a generalized gradient of an entire field line $\boldsymbol{r}(\lambda, \boldsymbol{r}_0)$ issuing from the reference point $\boldsymbol{r}_0$ for all λ. The difference vector $\boldsymbol{v}(\lambda, \boldsymbol{r}_0)$ represents the spatial shift at each λ along the particular field line $\boldsymbol{r}(\lambda, \boldsymbol{r}_0)$ to the corresponding point at λ along the neighboring field line $\boldsymbol{r}(\lambda, \boldsymbol{r}_0 + \boldsymbol{h})$ (see Figure 2); the components of $\boldsymbol{v}(\lambda, \boldsymbol{r}_0)$ are given by,

$$(\left.\boldsymbol{v}\right|_{\lambda, \boldsymbol{r}_0})^i := \sum_j (\left.\mathbf{F}\right|_{\lambda, \boldsymbol{r}_0})^i{}_j \, \boldsymbol{h}^j \tag{12}$$

For a given spatial variation $\boldsymbol{h}$, Equation (12) may be interpreted as a generalized directional derivative of an entire field line $\boldsymbol{r}(\lambda, \boldsymbol{r}_0)$ in the direction $\boldsymbol{v}(\lambda, \boldsymbol{r}_0)$. In other words, the spatial propagator $\mathbf{F}$ "propagates" every spatial variation $\boldsymbol{h}$ of the reference point $\boldsymbol{r}_0$ along the particular field line in 3D space.

$$v(\lambda, r_0) = F(\lambda, r_0) \cdot h$$

$$h = F(0, r_0) \cdot h = v(0, r_0)$$
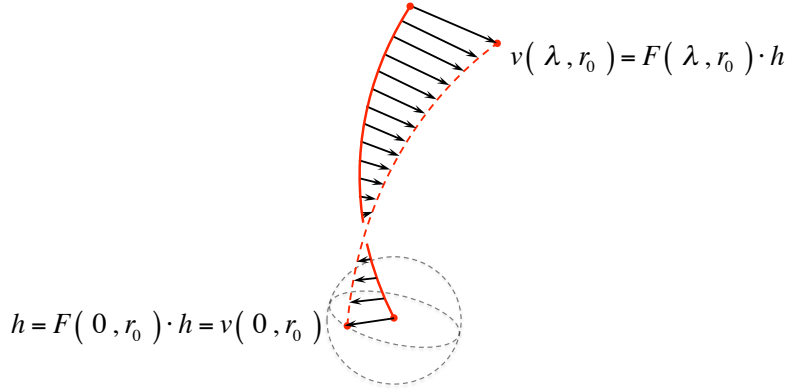
Figure 2. Illustration of the action of the spatial propagator. The spatial variation of a particular field line (solid red) in the direction $\boldsymbol{r}_0 \to \boldsymbol{r}_0 + \boldsymbol{h}$ is indicated by the dashed red line.

The matrix representation of the spatial propagator $\mathbf{F}(\lambda, \boldsymbol{r}_0)$ contains all the geometric information of the local congruence; that is, it carries the local geometric organization of the field lines within a neighborhood $\Omega_0 << h_m^3$ of a particular field line solution $\boldsymbol{r}(\lambda, \boldsymbol{r}_0)$. We give a precise meaning to this statement in Section 3.

2.3. Direct Relation Between the Spatial Propagator and the Vector Field

Like the field lines of the congruence, the spatial propagator $\mathbf{F}(\lambda, \boldsymbol{r}_0)$ is a function of both the connectivity parameter λ and reference point $\boldsymbol{r}_0$. In order to calculate the Propagator, one may integrate *all* the field lines, and then construct the difference Equation (10) between any two neighboring field lines, taking care to evaluate the scale length h_m for every field line. However, in typical physical

systems of interest the governing equations describe the evolution of the vector field (e.g., Faraday's Law, MHD induction, etc.), and the associated field lines are derived therefrom the solution. Hence, we seek a formulation of the spatial propagator directly from the vector field. Such a formulation for the calculation of a field line and its associated Propagator, allows the simultaneous calculation of the spatial behavior of *all* field lines within the h_m neighborhood.

To illustrate, we give a simple, qualitative derivation as follows. The connectivity parameter λ and the reference point $\boldsymbol{r}_0$ may be considered independent variables in the family of smooth integral curve solutions $\boldsymbol{r}\left(\lambda, \boldsymbol{r}_0\right)$ to the system of Equations (2) and (3). From this perspective, the spatial variation with respect to the reference point may be constructed from Equation (2) by

$$\frac{\partial}{\partial \boldsymbol{r}_0}\left(\frac{\partial \boldsymbol{r}\left(\lambda, \boldsymbol{r}_0\right)}{\partial \lambda}\right) = \frac{\partial}{\partial \boldsymbol{r}_0}\left(\boldsymbol{B}\left(\boldsymbol{r}\right)\right). \tag{13}$$

Since the vector field $\boldsymbol{B}\left(\boldsymbol{r}\right)$ is assumed to have smooth components, then the family of integral curve solutions $\boldsymbol{r}\left(\lambda, \boldsymbol{r}_0\right)$ is smooth in the variables λ and $\boldsymbol{r}_0$; hence, mixed partial derivatives commute, and (13) may be written

$$\frac{\partial}{\partial \lambda}\left(\frac{\partial \boldsymbol{r}\left(\lambda, \boldsymbol{r}_0\right)}{\partial \boldsymbol{r}_0}\right) = \left(\left.\frac{\partial \boldsymbol{B}\left(\boldsymbol{r}\right)}{\partial \boldsymbol{r}}\right|_{\boldsymbol{r}=\boldsymbol{r}\left(\lambda, \boldsymbol{r}_0\right)}\right) \cdot \left(\frac{\partial \boldsymbol{r}\left(\lambda, \boldsymbol{r}_0\right)}{\partial \boldsymbol{r}_0}\right). \tag{14}$$

By Equation (11), Equation (14) is a matrix evolution equation for the (unknown) spatial propagator $\mathbf{F}\left(\lambda, \boldsymbol{r}_0\right)$. Hence, the $\dfrac{\partial \boldsymbol{B}\left(\boldsymbol{r}\right)}{\partial \boldsymbol{r}}$ term is simply the rate of change of the vector field with respect to the spatial position $\boldsymbol{r} = \boldsymbol{r}\left(\lambda, \boldsymbol{r}_0\right)$; represented as a 3×3 matrix with respect to Cartesian basis,

$$\left(\left.\nabla \boldsymbol{B}\right|_{\boldsymbol{r}}\right)^i{}_j := \frac{\partial\left(\left.\boldsymbol{B}\right|_{\boldsymbol{r},t}\right)^i}{\partial \boldsymbol{r}^j} = \begin{pmatrix} \dfrac{\partial B^x}{\partial x} & \dfrac{\partial B^x}{\partial y} & \dfrac{\partial B^x}{\partial z} \\[2mm] \dfrac{\partial B^y}{\partial x} & \dfrac{\partial B^y}{\partial y} & \dfrac{\partial B^y}{\partial z} \\[2mm] \dfrac{\partial B^z}{\partial x} & \dfrac{\partial B^z}{\partial y} & \dfrac{\partial B^z}{\partial z} \end{pmatrix}, \tag{15}$$

where each partial derivative component is evaluated along the field line component functions, Equations (5).

Substituting Equations (11) and (15) into Equation (14), the spatial propagator $\mathbf{F}\left(\lambda, \boldsymbol{r}_0\right)$ satisfies the following first-order matrix differential equation; in components with respect to a Cartesian basis $\{\boldsymbol{e}_x, \boldsymbol{e}_y, \boldsymbol{e}_z\}$,

$$\frac{\partial\left(\left.\mathbf{F}\right|_{\lambda, \boldsymbol{r}_0}\right)^i{}_j}{\partial \lambda} = \sum_k \left(\left.\nabla \boldsymbol{B}\right|_{\boldsymbol{r}}\right)^i{}_k \left(\left.\mathbf{F}\right|_{\lambda, \boldsymbol{r}_0}\right)^k{}_j, \tag{16}$$

$$\left(\left.\mathbf{F}\right|_{0, \boldsymbol{r}_0}\right)^i{}_j = \delta^i{}_j, \tag{17}$$

where $\delta^i{}_j$ is the Kronecker delta.

We remark, by Equation (4) the matrix ODE, Equation (16), is the Lie transport (see e.g., Kobayashi & Nomizu, 1963, p. 29) of the propagated shift vector $\boldsymbol{v}$ along the vector field $\boldsymbol{B}$,

$$\mathcal{L}_{\boldsymbol{B}}\left(\boldsymbol{v}\right) = \boldsymbol{0} \tag{18}$$

where the reference shift vector $\boldsymbol{h}$ is a constant vector independent of the coordinates; that is $\left(\boldsymbol{B} \cdot \nabla\right)\mathbf{h} = \boldsymbol{0}$.

In general, Equations (2) and (16), along with their respective initial conditions (3) and (17), are generally referred to as the *equations of variation* (see e.g., Arnold, 1992, p. 223-225), and constitute a well-posed problem. Hence, the spatial propagator $\mathbf{F}\left(\lambda, \boldsymbol{r}_0\right)$ solution exists and is unique for all λ and $\boldsymbol{r}_0$ (see e.g., Bernstein, 2018, p. 1193-1195, for existence and uniqueness proof).

For any reference point $\boldsymbol{r}_0$ and all λ, the congruence of scale h_m is a particular solution to the equations of variation consisting of both the integral curve, $\boldsymbol{r}\left(\lambda, \boldsymbol{r}_0\right)$, and corresponding spatial propagator, $\mathbf{F}\left(\lambda, \mathbf{r}_0\right)$. The congruence may be interpreted as a local phase space of scale h_m for the field line connectivity consisting of elements $\boldsymbol{r}\left(\lambda, \boldsymbol{r}_0\right)$ and $\mathbf{F}\left(\lambda, \mathbf{r}_0\right)$ whose dynamics follow naturally from $\boldsymbol{B}\left(t, \boldsymbol{r}\right)$ and $\nabla\boldsymbol{B}\left(t, \boldsymbol{r}\right)$. With respect to the global Cartesian coordinates, these phase space elements are represented by a 3-component vector and 3×3-component matrix,

$$\boldsymbol{r}\left(\lambda, \boldsymbol{r}_0\right) = \sum_i \left(\left.\boldsymbol{r}\right|_{\lambda, \boldsymbol{r}_0}\right)^i \boldsymbol{e}_i,$$

$$\mathbf{F}\left(\lambda, \boldsymbol{r}_0\right) = \sum_{i,j}\left(\left.\mathbf{F}\right|_{\lambda, \boldsymbol{r}_0}\right)^i{}_j \, \boldsymbol{e}_i \otimes \boldsymbol{e}^j, \tag{19}$$

where $\{\boldsymbol{e}_x, \boldsymbol{e}_y, \boldsymbol{e}_z\}$ are the orthonormal basis vectors, and $\{\boldsymbol{e}^x, \boldsymbol{e}^y, \boldsymbol{e}^z\}$ the dual basis (see Appendix B.1).

2.4. General Representations of the Spatial Propagator

There are two fundamental representation categories of the spatial propagator $\mathbf{F}\left(\lambda, \boldsymbol{r}_0\right)$: the matrix representation with respect to a particular basis set $\boldsymbol{e}_i$, and the representation with respect to the connectivity parameter λ.

First, we consider the basis representation of the congruence; that is the field line $\boldsymbol{r}\left(\lambda, \boldsymbol{r}_0\right)$ and associated spatial propagator $\mathbf{F}\left(\lambda, \boldsymbol{r}_0\right)$ are, respectively a 3-component vector and 3×3 matrix representation *constructed with respect to a particular basis set.* Fundamentally, the matrix representation of the congruence *follows from* the vector field $\boldsymbol{B}\left(\boldsymbol{r}\right)$ and the $\nabla\boldsymbol{B}\left(\boldsymbol{r}\right)$ matrix; that is constructing $\boldsymbol{B}$ and $\nabla\boldsymbol{B}$ with respect to Cartesian basis vectors lead to the Cartesian representation of the congruence, Equations (19).

In the Cartesian representation, the basis vectors are independent of the spatial position and hence Equations (11) and (15) find a particularly simple form. However, general curvilinear basis vectors are position dependent; for example, consider spherical-polar orthonormal coordinate basis vectors,

$$\hat{\boldsymbol{e}}_r\left(\theta, \phi\right) = \sin\theta\cos\phi \, \boldsymbol{e}_x + \sin\theta\sin\phi \, \boldsymbol{e}_y + \cos\theta \, \boldsymbol{e}_z$$

$$\begin{aligned}
\hat{\boldsymbol{e}}_\theta\left(\theta,\phi\right) &= \cos\theta\cos\phi\,\boldsymbol{e}_x + \cos\theta\sin\phi\,\boldsymbol{e}_y - \sin\theta\,\boldsymbol{e}_z \\
\hat{\boldsymbol{e}}_\phi\left(\theta,\phi\right) &= -\sin\phi\,\boldsymbol{e}_x + \cos\phi\,\boldsymbol{e}_y,
\end{aligned} \tag{20}$$

prevalent within solar and space physics. Hence, in order to incorporate the spatial position dependence of general curvilinear basis vectors in this formulation, we *impose the condition that the spatial propagator* $\mathbf{F}\left(\lambda,\boldsymbol{r}_0\right)$ *transform as a tensor under general coordinate transformations.*

The tensor-condition requires the $\nabla\boldsymbol{B}\left(\boldsymbol{r}\right)$ object to be the matrix representation of the covariant differential of the vector field (see e.g., Kobayashi & Nomizu, 1963, p. 143-144). The components of the matrix representation of the covariant differential of the vector field with respect to general local curvilinear coordinates q^i is given by,

$$\left(\left.\nabla\boldsymbol{B}\right|_{\boldsymbol{r}}\right)^i{}_j = \frac{\partial}{\partial q^j}\left(\left.\boldsymbol{B}\right|_{\boldsymbol{r}}\right)^i + \sum_k\left(\left.\Gamma\right|_{\boldsymbol{r}}\right)^i{}_{jk}\left(\left.\boldsymbol{B}\right|_{\boldsymbol{r}}\right)^k \tag{21}$$

(see Appendix B.1 for derivation and discussion). The first term is simply the rate of change of the component functions with respect to the local coordinates. The coefficients $\left(\left.\Gamma\right|_{\boldsymbol{r}}\right)^i{}_{jk}$ in the second term account for the spatial position dependence of the basis vectors $\boldsymbol{q}_i\left(q^j\right)$. Equation (16) with (21), and initial condition (17), generalizes the field line deviation to general curvilinear coordinates (see e.g., Tassev & Savcheva, 2017; Scott et al., 2017, for application). In Appendices B.2 and B.3, we develop explicit matrix representations of the covariant differential of the vector field $\nabla\boldsymbol{B}\left(\boldsymbol{r}\right)$ with respect to the common spherical-polar bases used by the solar and space physics community (see e.g., Tassev & Savcheva, 2017).

Second, we consider the connectivity parameter representation of the congruence. For a given vector field $\boldsymbol{B}\left(\boldsymbol{r}\right)$, the congruence solution to Equations (2) and (16) with respect to λ is said to be given in the *natural representation*. That is the connectivity parameter λ has units of arc length per vector field magnitude, and the congruence, $\boldsymbol{r}\left(\lambda,\boldsymbol{r}_0\right)$ and $\mathbf{F}\left(\lambda,\boldsymbol{r}_0\right)$, reflects this functional dependence.

Recall the end of Section 2.1, the congruence represents an equivalence class under general affine transformations of the connectivity parameter, $\lambda\mapsto\ell\left(\lambda\right) = f\left(\boldsymbol{r}\right)\lambda + b$ for smooth, positive definite functions $f\left(\boldsymbol{r}\right)$ and scalar b. Hence, the matrix differential Equations (16) and (17) transform accordingly; with respect to Cartesian coordinates

$$\frac{\partial\left(\left.\mathbf{F}\right|_{\ell,\boldsymbol{r}_b}\right)^i{}_j}{\partial\ell} = \sum_k\left(\left(\left.\nabla\boldsymbol{X}\right|_{\boldsymbol{r}}\right)^i{}_k + \frac{\left(\left.\boldsymbol{X}\right|_{\boldsymbol{r}}\right)^i}{f\left(\boldsymbol{r}\right)}\frac{\partial f\left(\boldsymbol{r}\right)}{\partial r^k}\right)\left(\left.\mathbf{F}\right|_{\ell,\boldsymbol{r}_b}\right)^k{}_j, \tag{22}$$

$$\left(\left.\mathbf{F}\right|_{b,\boldsymbol{r}_b}\right)^i{}_j = \delta^i{}_j. \tag{23}$$

where $\boldsymbol{X}\left(\boldsymbol{r}\right) = \boldsymbol{B}\left(\boldsymbol{r}\right)\,/\,f\left(\boldsymbol{r}\right)$, and the positions are evaluated along $\boldsymbol{r} = \boldsymbol{r}\left(\ell,\boldsymbol{r}_b\right)$. Equation (22) with initial condition (23), generalizes the field line deviation to include affine transformations in the connectivity parameter representations (see e.g., Tassev & Savcheva, 2017; Scott et al., 2017).

Explicitly, recall the arc length representation example, Equations (8) and (9), with $f\left(\boldsymbol{r}\right) = \left|\boldsymbol{B}\left(\boldsymbol{r}\right)\right|$, and $\left|\boldsymbol{B}\left(\boldsymbol{r}\right)\right| \neq 0$. The vector field $\boldsymbol{X}\left(\boldsymbol{r}\right) = \hat{\boldsymbol{b}}\left(\boldsymbol{r}\right)$ is well

defined and identified with the unit magnetic field direction. In this example, arc length representation of the spatial propagator with respect to Cartesian coordinates satisfies

$$\frac{\partial\,(\,\mathbf{F}|_{\ell,\boldsymbol{r}_0}\,)^i{}_j}{\partial\ell} \;=\; \sum_k \left(\,(\,\nabla\hat{\boldsymbol{b}}|_{\boldsymbol{r}}\,)^i{}_k + \frac{(\,\hat{\boldsymbol{b}}|_{\boldsymbol{r}}\,)^i}{|\boldsymbol{B}\,(\boldsymbol{r})\,|}\,\frac{\partial|\boldsymbol{B}\,(\boldsymbol{r})\,|}{\partial r^k}\, \right)(\,\mathbf{F}|_{\ell,\boldsymbol{r}_0}\,)^k{}_j, \quad (24)$$

$$(\,\mathbf{F}|_{0,\boldsymbol{r}_0}\,)^i{}_j \;=\; \delta^i{}_j. \quad\quad (25)$$

where the positions are evaluated along arc length representation of the field line, $\boldsymbol{r} = \boldsymbol{r}\,(\ell,\boldsymbol{r}_0)$.

In the application to solar magnetic fields, constructing the congruence solution from data (e.g., SDO AIA 171) requires the solutions to Equations (8) and (24), with initial conditions (7) and (25), respectively. From this perspective, we have decoupled the magnetic field strength estimation from the field line trajectory estimation in the construction of the Propagator.

3. Geometric Deformation of a Congruence

Geometry describes the measurable lengths and angles associated with the system configuration. The interest of this congruence formalism is that all the geometric behavior of a local bundle of field lines is contained within a single integration of Equations (2) and (16), along with their respective initial conditions (3) and (17). The field line and corresponding spatial propagator implicitly incorporates all geometric information of the local bundle, via the vector magnetic field structure, $\boldsymbol{B}$ and $\nabla\boldsymbol{B}$. The generic geometric configuration of the congruence may be described by a combination of dilation (Section 3.1), stretch and rotation (Section 3.2), and gradients in the connectivity structure (Section 3.3).

We recall that by assumption the vector field components are smooth functions. Hence, by standard theorems of existence, uniqueness, and extension for ordinary differential equations (see e.g., Hirsch & Smale, 1974; Arnold, 1992; Taylor, 1996), each field line reference point $\boldsymbol{r}_0 \in \Omega_0$ is mapped smoothly and uniquely to the point $\boldsymbol{r} = \boldsymbol{r}\,(\lambda,\boldsymbol{r}_0) \in \Omega_\lambda$ (see Figure 1); that is, the neighborhood volume Ω_0 is mapped, smoothly and uniquely to the neighborhood volume Ω_λ. Hence, *the geometric deformation of the local congruence is reflected in the deformation of the initial volume Ω_0 by propagation along the congruence into Ω_λ.*

3.1. Congruence Dilation and the Determinant of the Spatial Propagator.

The dilation of a congruence is the compression/expansion of the constituent field lines, and is completely described by the determinant of the 3×3, non-singular (invertible) matrix representation of the spatial propagator $\mathbf{F}\,(\lambda,\boldsymbol{r}_0)$. This type of geometric deformation is quantified by the dilation of a volume $\Omega_\lambda \subseteq \mathbb{R}^3$ propagated through each λ along the congruence. In this section, we

make explicit the functional dependence of the deformed volume on both the λ parameter and the reference point $\boldsymbol{r}_0$, by denoting $\Omega_\lambda = \Omega(\lambda, \boldsymbol{r}_0)$.

The signed differential volume element in Cartesian coordinates is constructed from the coordinate differentials $\mathrm{d}x^i \, \boldsymbol{e}_i$,

$$\mathrm{d}^3\boldsymbol{x} = (\mathrm{d}z \, \boldsymbol{e}_z) \cdot (\, (\mathrm{d}x \, \boldsymbol{e}_x) \times (\mathrm{d}y \, \boldsymbol{e}_y) \,) = \boldsymbol{e}_z \cdot (\, \boldsymbol{e}_x \times \boldsymbol{e}_y \,) \, \mathrm{d}x \, \mathrm{d}y \, \mathrm{d}z. \qquad (26)$$

We may choose differential reference shift vectors to coincide with the Cartesian coordinate differentials $\mathrm{d}\boldsymbol{h}^i := \mathrm{d}x^i \, \boldsymbol{e}_i$, and hence write the *local signed differential volume element at the reference point*, $\mathrm{d}\Omega(0, \boldsymbol{r}_0) = \mathrm{d}^3\boldsymbol{x}$.

Each differential reference shift vector $\mathrm{d}\boldsymbol{h}^i$ may be propagated along the congruence under the action of $\mathbf{F}(\lambda, \boldsymbol{r}_0)$ (see Figure 3), such that

$$\mathrm{d}\boldsymbol{v}^i(\lambda, \boldsymbol{r}_0) \;=\; \mathbf{F}(\lambda, \boldsymbol{r}_0) \cdot \mathrm{d}\boldsymbol{h}^i = \mathrm{d}x^i \, \mathbf{F}(\lambda, \boldsymbol{r}_0) \cdot \boldsymbol{e}_i, \qquad (27)$$

where for each $i = x, y, z$, the $\mathbf{F}(\lambda, \boldsymbol{r}_0) \cdot \boldsymbol{e}_i$ is a vector; expanded with respect to Cartesian basis (see Appendix C.1),

$$\mathbf{F}(\lambda, \boldsymbol{r}_0) \cdot \boldsymbol{e}_i \;=\; (\, \mathbf{F}|_{\lambda, \boldsymbol{r}_0} \,)^x{}_i \, \boldsymbol{e}_x + (\, \mathbf{F}|_{\lambda, \boldsymbol{r}_0} \,)^y{}_i \, \boldsymbol{e}_y + (\, \mathbf{F}|_{\lambda, \boldsymbol{r}_0} \,)^z{}_i \, \boldsymbol{e}_z. \qquad (28)$$

Hence, the *local signed differential volume element propagated along the congruence* is completely determined by the action of the spatial propagator on the basis vectors,

$$\begin{aligned}
\mathrm{d}\Omega(\lambda, \boldsymbol{r}_0) \;&=\; \mathrm{d}\boldsymbol{v}^z(\lambda, \boldsymbol{r}_0) \cdot (\, \mathrm{d}\boldsymbol{v}^x(\lambda, \boldsymbol{r}_0) \times \mathrm{d}\boldsymbol{v}^y(\lambda, \boldsymbol{r}_0) \,) \\
&=\; (\, \mathbf{F}(\lambda, \boldsymbol{r}_0) \cdot \boldsymbol{e}_z \,) \cdot (\, (\, \mathbf{F}(\lambda, \boldsymbol{r}_0) \cdot \boldsymbol{e}_x \,) \times (\, \mathbf{F}(\lambda, \boldsymbol{r}_0) \cdot \boldsymbol{e}_y \,) \,) \, \mathrm{d}x \, \mathrm{d}y \, \mathrm{d}z.
\end{aligned}$$
$$(29)$$

By a standard result from vector calculus in three dimensions, the ratio of propagated volume element to initial volume element is given by the determinant of the matrix representation of $\mathbf{F}(\lambda, \boldsymbol{r}_0)$,

$$\begin{aligned}
\frac{\mathrm{d}\Omega(\lambda, \boldsymbol{r}_0)}{\mathrm{d}\Omega(0, \boldsymbol{r}_0)} \;&=\; \frac{(\, \mathbf{F}(\lambda, \boldsymbol{r}_0) \cdot \boldsymbol{e}_z \,) \cdot (\, (\, \mathbf{F}(\lambda, \boldsymbol{r}_0) \cdot \boldsymbol{e}_x \,) \times (\, \mathbf{F}(\lambda, \boldsymbol{r}_0) \cdot \boldsymbol{e}_y \,) \,)}{\boldsymbol{e}_z \cdot (\, \boldsymbol{e}_x \times \boldsymbol{e}_y \,)}, \\
&=\; \det \mathbf{F}(\lambda, \boldsymbol{r}_0). \qquad (30)
\end{aligned}$$

In Appendix C.1, we calculate Equation (30) explicitly for Cartesian basis. Furthermore, identity (30) is valid for arbitrary orthonormal basis sets (see e.g., Nickerson et al., 1959, p. 95-97, for standard treatment). From a geometric perspective, the determinant of the 3×3 matrix representation of $\mathbf{F}(\lambda, \boldsymbol{r}_0)$ acts as the Jacobian in a change of basis for the signed volume element propagated along the congruence (see Figure 3).

Since the differential reference shift vectors $\mathrm{d}\boldsymbol{h}^i$ are mapped under the action of the Propagator into the propagated differential vectors $\mathrm{d}\boldsymbol{v}^i(\lambda, \boldsymbol{r}_0)$, the signed differential volume elements $\mathrm{d}\Omega(0, \boldsymbol{r}_0)$ and $\mathrm{d}\Omega(\lambda, \boldsymbol{r}_0)$ are centered on the respective points $\boldsymbol{r}_0 = \boldsymbol{r}(0, \boldsymbol{r}_0)$ and $\boldsymbol{r} = \boldsymbol{r}(\lambda, \boldsymbol{r}_0)$. Hence, 3D integration with respect to the volume measure $\mathrm{d}\Omega(\lambda, \boldsymbol{r}_0)$ generates a total volume $\Omega(\lambda, \boldsymbol{r}_0)$, deformed with respect to the initial shape $\Omega(0, \boldsymbol{r}_0)$, and centered on the field line $\boldsymbol{r}(\lambda, \boldsymbol{r}_0)$
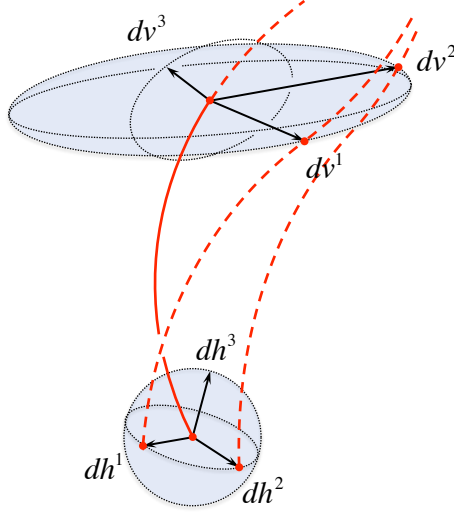
Figure 3. Illustration of the volumetric propagation under the action of the spatial propagator. Each dh_i is propagated to dv_i. The propagated vectors illustrated are linearly independent, and otherwise completely general.

at each value of λ. Moreover, by Equation (30) the deformed total volume at every λ may be caste as an integral with respect to the reference volume measure $d\Omega\left(0, \boldsymbol{r}_0\right)$ at the reference point $\boldsymbol{r}_0 = \boldsymbol{r}\left(0, \boldsymbol{r}_0\right)$,

$$\Omega\left(\lambda, \boldsymbol{r}_0\right) = \int_{\Omega(\lambda, \boldsymbol{r}_0)} d\Omega\left(\lambda, \boldsymbol{r}_0\right) = \int_{\Omega(0, \boldsymbol{r}_0)} \det \mathbf{F}\left(\lambda, \boldsymbol{r}_0\right) \; d\Omega\left(0, \boldsymbol{r}_0\right). \tag{31}$$

The dilation of the total volume $\Omega\left(\lambda, \boldsymbol{r}_0\right)$ by propagation along the congruence is completely determined by the determinant of the Propagator $\det \mathbf{F}\left(\lambda, \boldsymbol{r}_0\right)$ at each λ. Geometrically, the total volume $\Omega\left(\lambda, \boldsymbol{r}_0\right)$ decreases (volumetric compression) for $0 < \det \mathbf{F}\left(\lambda, \boldsymbol{r}_0\right) < 1$, remains constant (isochoric propagation) for $\det \mathbf{F}\left(\lambda, \boldsymbol{r}_0\right) = 1$, or increases (volumetric expansion) for $\det \mathbf{F}\left(\lambda, \boldsymbol{r}_0\right) > 1$, respectively.

We remark, $\det \mathbf{F}\left(\lambda, \boldsymbol{r}_0\right) < 0$ corresponds to a mapping from proper right-handed basis set, to a left-handed basis set. Such an $\mathbf{F}\left(\lambda, \boldsymbol{r}_0\right)$ is discontinuous and requires singularities in the vector field $\boldsymbol{B}$, which we do not consider in this work.

Moreover, using Equation (31), we can quantify the rate of volumetric dilation by propagation along the congruence,

$$\begin{aligned} \frac{\partial \Omega\left(\lambda, \boldsymbol{r}_0\right)}{\partial \lambda} &= \int_{\Omega(0, \boldsymbol{r}_0)} \frac{\partial \det \mathbf{F}\left(\lambda, \boldsymbol{r}_0\right)}{\partial \lambda} \; d\Omega\left(0, \boldsymbol{r}_0\right), \\ &= \int_{\Omega(0, \boldsymbol{r}_0)} \mathrm{Tr}\left(\; \nabla \boldsymbol{B}\left(\boldsymbol{r}\right)\;\right) \det \mathbf{F}\left(\lambda, \boldsymbol{r}_0\right) d\Omega\left(0, \boldsymbol{r}_0\right) \end{aligned} \tag{32}$$

Where we have made use of the identity,

$$\frac{\partial \det \mathbf{F}(\lambda, \boldsymbol{r}_0)}{\partial \lambda} = \mathrm{Tr}\left(\nabla \boldsymbol{B}(\boldsymbol{r})\right) \det \mathbf{F}(\lambda, \boldsymbol{r}_0), \tag{33}$$

(see Appendix C.2 for derivation).

In Equations (32) and (33), the $\mathrm{Tr}\left(\nabla \boldsymbol{B}(\boldsymbol{r})\right)$ term is evaluated at each point $\boldsymbol{r} = \boldsymbol{r}(\lambda, \boldsymbol{r}_0)$. In particular, every physical magnetic vector field is everywhere divergence-free, $\mathrm{Tr}\left(\nabla \boldsymbol{B}(\boldsymbol{r})\right) = \nabla \cdot \boldsymbol{B}(\boldsymbol{r}) = 0$ for all $\boldsymbol{r}$ and t. Then for all finite λ, by Equations (17) and (33),

$$\det \mathbf{F}(\lambda, \boldsymbol{r}_0) = \det \mathbf{F}(0, \boldsymbol{r}_0) = \det \mathbf{I} = 1, \tag{34}$$

which in turn implies the total volume is conserved under propagation along a congruence; that is, $\Omega(\lambda, \boldsymbol{r}_0) = \Omega(0, \boldsymbol{r}_0)$ is constant regardless of deformation. *Hence, we identify* $\det \mathbf{F}(\lambda, \boldsymbol{r}_0) = 1$ *for all* λ *and every* $\boldsymbol{r}_0$ *as the simplest topological invariant of a congruence generated by a smooth magnetic vector field, reflecting the divergence-free condition of physical magnetic fields.*

3.2. Congruence Stretch and Rotation and the Singular Value Decomposition of the Spatial Propagator.

The anisotropic stretch and rigid body rotation of a congruence are equivalent to the kinematic description of the propagated volume undergoing similar deformation; that is, the λ-evolution of the propagated vectors $\boldsymbol{v}(\lambda, \boldsymbol{r}_0)$ with respect to a local volume-centered orthogonal reference frame. The congruence stretch and rotation is mirrored in the change in length of the basis vectors, scaled by the deformation of the volume, and the rigid body rotation of these mutually orthogonal axes. This basic geometric picture is illustrated in Figure 4.

We seek a geometric description in which the orthogonality of the reference frame is preserved under rotation and the lengths of the direction vectors are scaled. This description initially suggests the λ-evolution of the eigen-decomposition of the spatial propagator matrix $\mathbf{F}$, in which the eigenvalues and eigenvectors play the role of scale factors and basis directions. The eigenvalues for a general, non-singular, 3×3 matrix $\mathbf{F}$ are determined by a cubic polynomial with real coefficients, the roots of which may be real or complex-valued depending the sign of the classical cubic discriminant. In the case of non-negative cubic discriminant, the eigenvalues are all real (perhaps with multiplicity > 1), the geometric interpretation is scaling along linearly independent eigenvectors (since $\mathbf{F}$ is a non-singular matrix). However, *mutual orthogonality of the eigenvectors follows only in the special case that the spatial propagator matrix is symmetric*, $\mathbf{F} = \mathbf{F}^T$ (where $\mathbf{F}^T$ denotes the matrix transpose). Moreover, a negative cubic discriminant corresponds to complex-valued eigenvalues and eigenvectors, the geometric interpretation of which is not a stretch and rotation of the propagated volume. Hence, the eigen-decomposition of the spatial propagator $\mathbf{F}$ does not provide the correct stretch and rotation description.

To determine the correct description, consider that a general stretch is described by a *change in the length* of propagated vectors $\boldsymbol{v}(\lambda, \boldsymbol{r}_0)$ within the

$$r = r\left(\lambda, r_0\right)$$

$$r_0 = r\left(0, r_0\right)$$
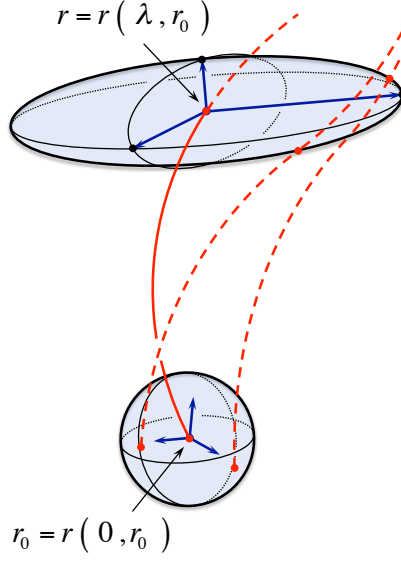
Figure 4. Illustration of an anisotropic stretch and rigid body rotation of an orthogonal frame centered about the central field line trajectory $r\left(\lambda, r_0\right)$ within the propagated volume. At the difference of Figure 3, a specific orthonormal frame, $\hat{r}_\alpha$, is shown centered on $r\left(0, r_0\right)$. It is rotated along the central field line into the specific orthonormal frame, $\hat{l}_\alpha$, centered at $r\left(\lambda, r_0\right)$ while the vector lengths are simultaneously scaled by the corresponding σ_α as defined in Section 3.2.

propagated volume. The length of a vector is described by the norm,

$$
\begin{aligned}
\left|v\left(\lambda, r_0\right)\right| &= \left(v\left(\lambda, r_0\right) \cdot v\left(\lambda, r_0\right)\right)^{1/2} \\
&= \left(h \cdot \mathbf{F}^T\left(\lambda, r_0\right) \cdot \mathbf{F}\left(\lambda, r_0\right) \cdot h\right)^{1/2} .
\end{aligned}
\tag{35}
$$

Equation (35) is a real-valued function of λ that involves the symmetric matrix $\mathbf{F}^T \cdot \mathbf{F}$, as opposed to the spatial propagator $\mathbf{F}$ alone. By a standard theorem of linear algebra (see e.g., Halmos, 1958, section 79), the eigenvalues of the symmetric matrix $\mathbf{F}^T \cdot \mathbf{F}$ are all real (possibly with multiplicity > 1), and the eigenvectors are everywhere mutually orthogonal. More generally, the symmetric matrices $\mathbf{F}^T \cdot \mathbf{F}$ and $\mathbf{F} \cdot \mathbf{F}^T$ have identical eigenvalues, as well as orthonormal, albeit different, eigenvector bases. Hence, for a general, non-singular spatial propagator $\mathbf{F}$, the real eigenvalues and real orthogonal eigenvectors of the symmetric matrices $\mathbf{F} \cdot \mathbf{F}^T$, respectively $\mathbf{F}^T \cdot \mathbf{F}$, may be used to infer indirectly the geometric stretch and rotation interpretation of $\mathbf{F}$.

Formally, for each fixed r_0 and all λ, there exists a factorization of $\mathbf{F}\left(\lambda, r_0\right)$, called the *Singular Value Decomposition* (SVD), given by

$$
\mathbf{F}\left(\lambda, r_0\right) = \mathbf{R}_l\left(\lambda, r_0\right) \cdot \mathbf{D}\left(\lambda, r_0\right) \cdot \mathbf{R}_r\left(\lambda, r_0\right),
\tag{36}
$$

where $\mathbf{D}\left(\lambda, r_0\right)$ is a 3×3 diagonal matrix, and the $\mathbf{R}_l\left(\lambda, r_0\right)$ and $\mathbf{R}_r\left(\lambda, r_0\right)$ are 3×3 orthogonal matrices (e.g., Bernstein, 2018, p. 555 - 558). The diagonal

entries of the matrix $\mathbf{D}\left(\lambda, \boldsymbol{r}_0\right)$ are non-negative functions $\sigma_\alpha\left(\lambda, \boldsymbol{r}_0\right)$ for $\alpha = 1, 2, 3$, given by

$$\sigma_\alpha\left(\lambda, \boldsymbol{r}_0\right) = \sqrt{q_\alpha\left(\lambda, \boldsymbol{r}_0\right)}, \tag{37}$$

where $q_\alpha\left(\lambda, \boldsymbol{r}_0\right)$ are the eigenvalues of the matrices $\mathbf{F}^T \cdot \mathbf{F}$ and $\mathbf{F} \cdot \mathbf{F}^T$. The columns of $\mathbf{R}_l\left(\lambda, \boldsymbol{r}_0\right)$, denoted by $\hat{\boldsymbol{l}}_\alpha\left(\lambda, \boldsymbol{r}_0\right)$, are the mutually orthogonal eigenvectors of the symmetric matrix $\mathbf{F} \cdot \mathbf{F}^T$; respectively, the columns of $\mathbf{R}_r\left(\lambda, \boldsymbol{r}_0\right)$, denoted by $\hat{\boldsymbol{r}}_\alpha\left(\lambda, \boldsymbol{r}_0\right)$, are the mutually orthogonal eigenvectors of the symmetric matrix $\mathbf{F}^T \cdot \mathbf{F}$.

For each reference point $\boldsymbol{r}_0$ and fixed λ, the set of values σ_α for $\alpha = 1, 2, 3$ are called the *singular values* of $\mathbf{F}\left(\lambda, \boldsymbol{r}_0\right)$, and the corresponding set of vectors $\hat{\boldsymbol{l}}_\alpha$ and $\hat{\boldsymbol{r}}_\alpha$ are called the *singular vectors* of $\mathbf{F}\left(\lambda, \boldsymbol{r}_0\right)$. The anisotropic stretch and rigid rotation of the propagated volume, equivalently the congruence geometry, is completely determined by the singular values and singular vectors of the spatial propagator $\mathbf{F}\left(\lambda, \boldsymbol{r}_0\right)$. Geometrically, an orthonormal frame $\hat{\boldsymbol{r}}_\alpha$ in the reference volume Ω_0 is rotated into the orthonormal frame $\hat{\boldsymbol{l}}_\alpha$ in the propagated volume Ω_λ while the vector lengths are simultaneously scaled by the corresponding σ_α as shown in Figure 4.

We may decompose this simultaneous stretch and rigid body rotation effect through a *Polar-Decomposition* of the spatial propagator. Since $\mathbf{R}_l\left(\lambda, \boldsymbol{r}_0\right)$ is an orthogonal matrix $\left(\mathbf{R}^{-1} = \mathbf{R}^T\right)$ for each $\boldsymbol{r}_0$ and all λ, then $\mathbf{R}_l^T\left(\lambda, \boldsymbol{r}_0\right) \cdot \mathbf{R}_l\left(\lambda, \boldsymbol{r}_0\right) = \mathbf{I}$, where $\mathbf{I}$ is the identity. Hence, we may rewrite Equation (36) as

$$
\begin{aligned}
\mathbf{F}\left(\lambda, \boldsymbol{r}_0\right) &= \mathbf{R}_l\left(\lambda, \boldsymbol{r}_0\right) \cdot \mathbf{D}\left(\lambda, \boldsymbol{r}_0\right) \cdot \mathbf{I} \cdot \mathbf{R}_r\left(\lambda, \boldsymbol{r}_0\right) \\
&= \mathbf{R}_l\left(\lambda, \boldsymbol{r}_0\right) \cdot \mathbf{D}\left(\lambda, \boldsymbol{r}_0\right) \cdot \left(\mathbf{R}_l^T\left(\lambda, \boldsymbol{r}_0\right) \cdot \mathbf{R}_l\left(\lambda, \boldsymbol{r}_0\right)\right) \cdot \mathbf{R}_r\left(\lambda, \boldsymbol{r}_0\right) \\
&= \left(\mathbf{R}_l\left(\lambda, \boldsymbol{r}_0\right) \cdot \mathbf{D}\left(\lambda, \boldsymbol{r}_0\right) \cdot \mathbf{R}_l^T\left(\lambda, \boldsymbol{r}_0\right)\right) \cdot \left(\mathbf{R}_l\left(\lambda, \boldsymbol{r}_0\right) \cdot \mathbf{R}_r\left(\lambda, \boldsymbol{r}_0\right)\right) \\
&= \mathbf{V}\left(\lambda, \boldsymbol{r}_0\right) \cdot \mathbf{R}\left(\lambda, \boldsymbol{r}_0\right). \tag{38}
\end{aligned}
$$

By the exact same arguments, making use of the orthogonality of $\mathbf{R}_r\left(\lambda, \boldsymbol{r}_0\right)$, we find an equivalent rewrite of Equation (36) as

$$\mathbf{F}\left(\lambda, \boldsymbol{r}_0\right) = \mathbf{R}\left(\lambda, \boldsymbol{r}_0\right) \cdot \mathbf{U}\left(\lambda, \boldsymbol{r}_0\right). \tag{39}$$

The equivalent decompositions (38), respectively (39), are referred to as the *left-polar decomposition*, respectively *right-polar decomposition*, of the spatial propagator (see e.g., Halmos, 1958, section 83). Unlike the general spatial propagator $\mathbf{F}\left(\lambda, \boldsymbol{r}_0\right)$ itself, the matrices $\mathbf{V}\left(\lambda, \boldsymbol{r}_0\right)$ and $\mathbf{U}\left(\lambda, \boldsymbol{r}_0\right)$, denoted respectively the *left-stretch* and *right-stretch*, are symmetric and positive-definite; these 3×3 matrices are defined by

$$
\begin{aligned}
\mathbf{V}\left(\lambda, \boldsymbol{r}_0\right) &:= \mathbf{R}_l\left(\lambda, \boldsymbol{r}_0\right) \cdot \mathbf{D}\left(\lambda, \boldsymbol{r}_0\right) \cdot \mathbf{R}_l^T\left(\lambda, \boldsymbol{r}_0\right), \\
\mathbf{U}\left(\lambda, \boldsymbol{r}_0\right) &:= \mathbf{R}_r^T\left(\lambda, \boldsymbol{r}_0\right) \cdot \mathbf{D}\left(\lambda, \boldsymbol{r}_0\right) \cdot \mathbf{R}_r\left(\lambda, \boldsymbol{r}_0\right). \tag{40}
\end{aligned}
$$

Moreover, the matrix $\mathbf{R}\left(\lambda, \boldsymbol{r}_0\right)$ is a 3×3, orthogonal matrix, and is defined by

$$\mathbf{R}\left(\lambda, \boldsymbol{r}_0\right) := \mathbf{R}_l\left(\lambda, \boldsymbol{r}_0\right) \cdot \mathbf{R}_r\left(\lambda, \boldsymbol{r}_0\right). \tag{41}$$

The left-stretch $\mathbf{V}\left(\lambda, \boldsymbol{r}_0\right)$, right-stretch $\mathbf{U}\left(\lambda, \boldsymbol{r}_0\right)$, and rotation $\mathbf{R}\left(\lambda, \boldsymbol{r}_0\right)$ matrices all naturally inherit their (global) coordinate representation from the matrix representation of the spatial propagator $\mathbf{F}\left(\lambda, \boldsymbol{r}_0\right)$.

Equations (40) represent two coordinate rotations, by the $\mathbf{R}_l\left(\lambda, \boldsymbol{r}_0\right)$ and $\mathbf{R}_r\left(\lambda, \boldsymbol{r}_0\right)$ matrices, that diagonalize the $\mathbf{V}\left(\lambda, \boldsymbol{r}_0\right)$ and $\mathbf{U}\left(\lambda, \boldsymbol{r}_0\right)$ matrices. The anisotropic stretch and rigid body rotation geometric interpretation, however, becomes explicit by application of the standard spectral decomposition theorem of linear algebra (see e.g., Halmos, 1958, section 79). Since the matrices $\mathbf{V}\left(\lambda, \boldsymbol{r}_0\right)$ and $\mathbf{U}\left(\lambda, \boldsymbol{r}_0\right)$ are symmetric, there exist orthonormal eigen-bases $\hat{\boldsymbol{l}}_\alpha\left(\lambda, \boldsymbol{r}_0\right)$, respectively $\hat{\boldsymbol{r}}_\alpha\left(\lambda, \boldsymbol{r}_0\right)$, with respect to which the matrix representations are

$$\mathbf{V}\left(\lambda, \boldsymbol{r}_0\right) \;=\; \sum_\alpha \; \sigma_\alpha\left(\lambda, \boldsymbol{r}_0\right) \; \hat{\boldsymbol{l}}_\alpha\left(\lambda, \boldsymbol{r}_0\right) \otimes \hat{\boldsymbol{l}}_\alpha\left(\lambda, \boldsymbol{r}_0\right),$$

$$\mathbf{U}\left(\lambda, \boldsymbol{r}_0\right) \;=\; \sum_\alpha \; \sigma_\alpha\left(\lambda, \boldsymbol{r}_0\right) \; \hat{\boldsymbol{r}}_\alpha\left(\lambda, \boldsymbol{r}_0\right) \otimes \hat{\boldsymbol{r}}_\alpha\left(\lambda, \boldsymbol{r}_0\right). \tag{42}$$

By Equations (40) and (41), the eigen-bases $\hat{\boldsymbol{l}}_\alpha\left(\lambda, \boldsymbol{r}_0\right)$, respectively $\hat{\boldsymbol{r}}_\alpha\left(\lambda, \boldsymbol{r}_0\right)$, of the left-stretch $\mathbf{V}\left(\lambda, \boldsymbol{r}_0\right)$, respectively right-stretch $\mathbf{U}\left(\lambda, \boldsymbol{r}_0\right)$, matrices are the singular vectors of the spatial propagator $\mathbf{F}\left(\lambda, \boldsymbol{r}_0\right)$.

Moreover, the singular vectors $\hat{\boldsymbol{l}}_\alpha\left(\lambda, \boldsymbol{r}_0\right)$ and $\hat{\boldsymbol{r}}_\alpha\left(\lambda, \boldsymbol{r}_0\right)$ are related via the rotation matrix $\mathbf{R}\left(\lambda, \boldsymbol{r}_0\right)$, Equation (41). By Equations (38) and (39), the Right and Left Polar decompositions are equal, and hence, $\mathbf{V} = \mathbf{R} \cdot \mathbf{U} \cdot \mathbf{R}^{-1}$. Moreover, using the eigen-basis representations (42), and the orthogonality of the rotation matrix $\mathbf{R}^{-1} = \mathbf{R}^T$, we find

$$\sum_\alpha \; \sigma_\alpha \; \hat{\boldsymbol{l}}_\alpha \otimes \hat{\boldsymbol{l}}_\alpha \;=\; \mathbf{R} \cdot \left(\sum_\alpha \sigma_\alpha \; \hat{\boldsymbol{r}}_\alpha \otimes \hat{\boldsymbol{r}}_\alpha \right) \cdot \mathbf{R}^T$$

$$= \sum_\alpha \; \sigma_\alpha \left(\; \mathbf{R} \cdot \hat{\boldsymbol{r}}_\alpha \; \right) \otimes \left(\; \hat{\boldsymbol{r}}_\alpha \cdot \mathbf{R}^T \; \right).$$

Hence, matching terms

$$\hat{\boldsymbol{l}}_\alpha\left(\lambda, \boldsymbol{r}_0\right) \;=\; \mathbf{R}\left(\lambda, \boldsymbol{r}_0\right) \cdot \hat{\boldsymbol{r}}_\alpha\left(\lambda, \boldsymbol{r}_0\right) = \hat{\boldsymbol{r}}_\alpha\left(\lambda, \boldsymbol{r}_0\right) \cdot \mathbf{R}^T\left(\lambda, \boldsymbol{r}_0\right). \tag{43}$$

Furthermore, inverting (43) yields,

$$\hat{\boldsymbol{r}}_\alpha\left(\lambda, \boldsymbol{r}_0\right) \;=\; \hat{\boldsymbol{l}}_\alpha\left(\lambda, \boldsymbol{r}_0\right) \cdot \mathbf{R}\left(\lambda, \boldsymbol{r}_0\right) = \mathbf{R}^T\left(\lambda, \boldsymbol{r}_0\right) \cdot \hat{\boldsymbol{l}}_\alpha\left(\lambda, \boldsymbol{r}_0\right). \tag{44}$$

Using Equations (42) and (44) in the Left Polar Decomposition (38), the spatial propagator $\mathbf{F}\left(\lambda, \boldsymbol{r}_0\right)$ matrix may be represented with respect to the singular vector basis $\hat{\boldsymbol{l}}_\alpha\left(\lambda, \boldsymbol{r}_0\right)$ and $\hat{\boldsymbol{r}}_\alpha\left(\lambda, \boldsymbol{r}_0\right)$,

$$\mathbf{F}\left(\lambda, \boldsymbol{r}_0\right) \;=\; \sum_\alpha \; \sigma_\alpha\left(\lambda, \boldsymbol{r}_0\right) \; \hat{\boldsymbol{l}}_\alpha\left(\lambda, \boldsymbol{r}_0\right) \otimes \hat{\boldsymbol{r}}_\alpha\left(\lambda, \boldsymbol{r}_0\right). \tag{45}$$

Geometrically, for each λ, the action of the matrices $\mathbf{V}\left(\lambda, \boldsymbol{r}_0\right)$ and $\mathbf{U}\left(\lambda, \boldsymbol{r}_0\right)$ is to scale the propagated volume by the singular values of the spatial propagator

$\mathbf{F}\left(\lambda, \boldsymbol{r}_0\right)$. Whereas, the action of the rotation matrix $\mathbf{R}\left(\lambda, \boldsymbol{r}_0\right)$ is to rotate the singular directions of the reference state Ω_0 to align with the singular directions of the propagated state Ω_λ (see Figure 5). Hence, *the symmetric matrices* $\mathbf{V}\left(\lambda, \boldsymbol{r}_0\right)$ *and* $\mathbf{U}\left(\lambda, \boldsymbol{r}_0\right)$ *characterize the anisotropic stretch of the propagated volume, and the orthogonal* $\mathbf{R}\left(\lambda, \boldsymbol{r}_0\right)$ *characterizes the smooth rigid body rotation of the propagated volume along the congruence.*
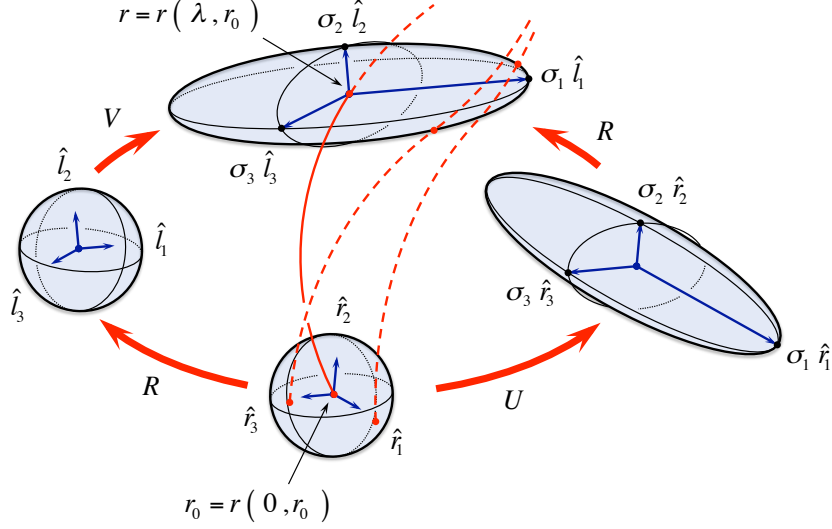
Figure 5. Illustration of the polar decomposition of the spatial propagator. The right polar decomposition, $\mathbf{F} = \mathbf{R} \cdot \mathbf{U}$, stretches/compresses by a factor of σ_α along the corresponding direction $\hat{\boldsymbol{r}}_\alpha$, followed by a rotation aligning with $\hat{\boldsymbol{l}}_\alpha$; the left polar decomposition, $\mathbf{F} = \mathbf{V} \cdot \mathbf{R}$, rotates $\hat{\boldsymbol{r}}_\alpha$ to align with $\hat{\boldsymbol{l}}_\alpha$, followed by a stretch/compression by a factor of σ_α along the corresponding direction $\hat{\boldsymbol{l}}_\alpha$.

We remark, the basis $\hat{\boldsymbol{l}}_\alpha\left(\lambda, \boldsymbol{r}_0\right)$ describes the singular axes of the stretched and rotated state Ω_λ. Similarly, for any λ the basis $\hat{\boldsymbol{r}}_\alpha\left(\lambda, \boldsymbol{r}_0\right)$ identify the singular axes of the stretched but un-rotated reference state Ω_0. Hence, for any λ the basis $\hat{\boldsymbol{r}}_\alpha\left(\lambda, \boldsymbol{r}_0\right)$ are the singular directions of the reference state Ω_0. However, a spherical reference state Ω_0 has no preferred directions; this follows from the fact that the initial condition $\mathbf{F}\left(0, \boldsymbol{r}_0\right) = \mathbf{I}$ possesses a single degenerate singular value (eigenvalue) $\sigma = 1$ of multiplicity 3. The resolution of this is that a unique, non-degenerate, orthonormal singular basis $\hat{\boldsymbol{r}}_\alpha\left(\lambda, \boldsymbol{r}_0\right)$ in the reference state Ω_0 always exists and *follows from* any spatial propagator $\mathbf{F}\left(\lambda, \boldsymbol{r}_0\right)$ with a non-degenerate singular values.

From a computational standpoint, since $\mathbf{F}$ is non-singular, the matrices $\mathbf{V}$, $\mathbf{U}$, and $\mathbf{R}$ may be determined directly from $\mathbf{F}$, $\mathbf{F} \cdot \mathbf{F}^T$, and $\mathbf{F}^T \cdot \mathbf{F}$. Using Equations (38), (39), and that $\mathbf{R}$ is an orthogonal matrix, $\mathbf{V}$, $\mathbf{U}$, and $\mathbf{R}$ follow immediately

$$
\begin{aligned}
\mathbf{V}\left(\lambda, \boldsymbol{r}_0\right) &= \sqrt{\mathbf{F}\left(\lambda, \boldsymbol{r}_0\right) \cdot \mathbf{F}^T\left(\lambda, \boldsymbol{r}_0\right)}\,, \\
\mathbf{U}\left(\lambda, \boldsymbol{r}_0\right) &= \sqrt{\mathbf{F}^T\left(\lambda, \boldsymbol{r}_0\right) \cdot \mathbf{F}\left(\lambda, \boldsymbol{r}_0\right)}\,, \\
\mathbf{R}\left(\lambda, \boldsymbol{r}_0\right) &= \mathbf{F}\left(\lambda, \boldsymbol{r}_0\right) \cdot \mathbf{U}^{-1}\left(\lambda, \boldsymbol{r}_0\right) = \mathbf{V}^{-1}\left(\lambda, \boldsymbol{r}_0\right) \cdot \mathbf{F}\left(\lambda, \boldsymbol{r}_0\right)\,.
\end{aligned}
\tag{46}
$$

Since the matrices $\mathbf{F} \cdot \mathbf{F}^T$ and $\mathbf{F}^T \cdot \mathbf{F}$ are diagonalizable with respect to their respective eigen-bases, the square root operation is well-defined.

We note, the left-stretch $\mathbf{V}(\lambda, \boldsymbol{r}_0)$, and right-stretch $\mathbf{U}(\lambda, \boldsymbol{r}_0)$, matrices are symmetric. However, it may be shown the full 3×3 matrix representation of the Spatial Propagator solution is *directly dependent* on the current distribution. Consider a quasi-static magnetic field $\boldsymbol{B}(\boldsymbol{r})$ with a non-trivial current distribution, $\boldsymbol{J}(\boldsymbol{r})$, which satisfies Ampere's Law, $\mu_0\,\boldsymbol{J}(\boldsymbol{r}) = \nabla \times \boldsymbol{B}(\boldsymbol{r})$. The covariant differential of the vector field $\nabla\boldsymbol{B}$ may be decomposed into symmetric and anti-symmetric parts,

$$(\left. \nabla\boldsymbol{B}\right|_{\boldsymbol{r}})^i{}_j \;=\; \frac{1}{2} \left((\left.\nabla\boldsymbol{B}\right|_{\boldsymbol{r}})^i{}_j + (\left.\nabla\boldsymbol{B}\right|_{\boldsymbol{r}}{}^T)^i{}_j \right) + \frac{\mu_0}{2} (\left.\mathbf{J}^\times\right|_{\boldsymbol{r}})^i{}_j. \quad (47)$$

where the superscript T denotes the matrix transpose. The matrix $\mathbf{J}^\times(\boldsymbol{r})$, denoted "J-supercross", is a 3×3 matrix representation of the current distribution (with respect to a Cartesian basis),

$$(\left.\mathbf{J}^\times\right|_{\boldsymbol{r}})^i{}_j \;:=\; \begin{pmatrix} 0 & J_z(\boldsymbol{r}) & -J_y(\boldsymbol{r}) \\ -J_z(\boldsymbol{r}) & 0 & J_x(\boldsymbol{r}) \\ J_y(\boldsymbol{r}) & -J_x(\boldsymbol{r}) & 0 \end{pmatrix}. \quad (48)$$

The Spatial Propagator governing matrix ODE (16) may be written,

$$\frac{\partial (\left.\mathbf{F}\right|_{\lambda,\boldsymbol{r}_0})^i{}_j}{\partial\lambda} \;=\; \frac{1}{2} \sum_k \left((\left.\nabla\boldsymbol{B}\right|_{\boldsymbol{r}})^i{}_k + (\left.\nabla\boldsymbol{B}\right|_{\boldsymbol{r}}{}^T)^i{}_k + \mu_0 (\left.\mathbf{J}^\times\right|_{\boldsymbol{r}})^i{}_k \right) (\left.\mathbf{F}\right|_{\lambda,\boldsymbol{r}_0})^k{}_j.$$
$$(49)$$

The initial condition (17) remains unchanged. We note, dropping the quasi-steady assumption leads to a similar ODE with the addition of a "supercross" displacement current density matrix term; we do not pursue such high-frequency dynamics here.

Hence, through Equation (49), the congruence rotation matrix, $\mathbf{R}(\lambda, \boldsymbol{r}_0)$, requires a non-trivial anti-symmetric part of the covariant differential, equivalently a non-trivial (parallel) current distribution $\boldsymbol{J}(\boldsymbol{r})$. Moreover, under reasonable conditions we identify a class of magnetic fields $\boldsymbol{B}(\boldsymbol{r})$ for which the rotation matrix $\mathbf{R}(\lambda, \boldsymbol{r}_0)$ depends *only* on the parallel current distribution $\boldsymbol{J}(\boldsymbol{r})$. Geometrically, the congruence rotation describes the twist of all neighboring integral curves about a central axis field line, and is therefore a measure of the twist-helicity. The relationship between the Spatial Propagator, rotation matrix, (twist-) magnetic helicity, and (parallel) current distribution is beyond the scope of this work.

3.3. Quasi-Separatrix Layers and the Q-Factor from the Spatial Propagator.

We have shown in the previous sections 3.1 and 3.2 that the congruence geometry is equivalent to the kinematics of a volume undergoing dilation, stretch deformation, and rigid body rotation under the action of the spatial propagator $\mathbf{F}(\lambda, \boldsymbol{r}_0)$.

A separatrix surface reflects the collapse of the 3D volume into a 2D surface as it is kinematically propagated by the congruence. The quasi-separatrix layer is therefore identified by the "extreme" kinematic deformation of near-collapse of the 3D volume; "extreme" being subjective and requiring a (user-defined) quantifier threshold.

We remark, recalling from Section 3.1 that the divergence-free condition for vector magnetic fields leads to the topological invariant, $\det \mathbf{F}(\lambda, \boldsymbol{r}_0) = 1$. Geometrically, the volumetric kinematics are incompressible; that is, the 3D shape deforms under the action of $\mathbf{F}(\lambda, \boldsymbol{r}_0)$ while the total volume remains constant. Compressible vector fields are outside the scope of this work. Hence, the separatrix surfaces in a vector magnetic field are described by infinite stretch deformation of the volume.

For a fixed reference point $\boldsymbol{r}_0$, the stretch deformation of a congruence in 3D at each λ is quantified by three non-negative singular values $\sigma_\alpha \in \mathbb{R}_{\geq 0}$ of the spatial propagator $\mathbf{F}(\lambda, \boldsymbol{r}_0)$. There is an inter-dependence between the singular values governed by the divergence-free condition. While the full algebraic proof is beyond the scope of this work, the singular values effectively reflect the eigenvalues structure of the $\nabla \mathbf{B}$ matrix. Hence, from a geometric perspective, the relative strengths of the set of singular values may be used to identify 3D quasi-separatrix layers (QSLs), 2D separatrix surfaces, 1D separator lines, and 0D null points within the field structure. The basic geometry follows as:

1. If any one singular value becomes zero, $\sigma_i \to 0$, then the other two correspondingly diverge to infinity, $\sigma_j, \sigma_k \to \infty$; geometrically, the 3D field line bundle has collapsed into a 2D surface.
2. If any two of the singular values become zero, $\sigma_i, \sigma_j \to 0$, then the remaining one correspondingly diverges to infinity, $\sigma_k \to \infty$; geometrically, the 3D field line bundle has collapsed into a 1D line.
3. The divergence-free condition prevents all three singular values from approaching zero simultaneously; geometrically, the 3D field line bundle cannot collapse to a 0D point.

For example, in the natural representation the fan surface, respectively spine line(s), associated with a magnetic null are identified by the vanishing of one, respectively two, singular values as $|\lambda| \to \infty$. More generally, however, it remains an open question regarding the identification of other non-trivial topologies which exhibit the vanishing of one or multiple singular values at finite and/or infinite $|\lambda|$.

Truly infinite singular values for σ_α determine 2D separatrix surfaces and 1D separator lines. "Extreme" singular values identify quasi-separatrix layers; that is, e.g., $\sigma_i \leq 1/\epsilon$ correspondingly $\sigma_j, \sigma_k \geq \epsilon$, for some user-defined threshold $\epsilon >> 1$. Analogous "extreme" threshold arguments may be made around separator lines.

Through this point, we have investigated the geometric meaning, consequences, and relations between the singular values of the full-3D Spatial Propagator in various limits. The QSL is often described in terms of the "squashing" of a flux tube (see e.g., Titov, 2007; Tassev & Savcheva, 2017; Scott et al., 2017);

essentially, a relational measure between the eccentricity of the flux tube cross-sectional area at the system boundaries, and hence is inherently 2D. Moreover, the squashing of a flux tube is defined entirely independent of rotation. For the remainder of this section, we demonstrate a dimensional reduction of the full-3D Spatial Propagator to describe the 2D squashing of the congruence. In particular, we demonstrate a simple construction the popular squashing factor, Q (Titov et al., 2002; Titov, 2007) from the Spatial Propagator. We note, our aim here is *neither* a reformulation or more efficient computation of the squashing factor, Q, over that which is available in the open literature (see e.g., Tassev & Savcheva, 2017). Rather the purpose is simply to show exactly how the popular Q-value may be derived from, and therefore fits as a small piece within this general context of the Spatial Propagator.

Throughout this work we have assumed that the vector magnetic field $\boldsymbol{B}\left(\boldsymbol{r}\right)$ has smooth component functions, Equations (1), that may be described with respect to a single global Cartesian coordinate chart. Hence the congruence solution components, Equations (19), described with respect to the same global Cartesian coordinate chart are also smooth, single-valued functions of the connectivity parameter λ, and reference condition coordinates $\boldsymbol{r}_0$. Furthermore, by construction, this framework is valid for any global coordinate chart which covers the system (see Appendix B.1 for general coordinate chart formulations, and Appendices B.2 and B.3 for spherical-polar formulations).

Consider for simplicity a smooth vector field $\boldsymbol{B}\left(\boldsymbol{r}\right)$ in a bounded Cartesian box; that is, we let the coordinate domains be $x \in [-L_x, L_x]$, $y \in [-L_y, L_y]$, and $z \in [-L_z, L_z]$. The (inward) unit normal $\hat{\boldsymbol{n}}$ at the boundaries is parallel (up to a sign) to the respective Cartesian basis vectors $\{\boldsymbol{e}_x, \boldsymbol{e}_y, \boldsymbol{e}_z\}$. Moreover, consider a congruence solution, Equations (19), with characteristic scale h_m, consistent with the given vector field $\boldsymbol{B}\left(\boldsymbol{r}\right)$, such that the reference point $\boldsymbol{r}_0$ is chosen at the $z = -L_z$ boundary, and the end point $\boldsymbol{r}\left(L, \boldsymbol{r}_0\right)$ follows on the $z = L_z$ boundary (see Figure 6).

Recall from Section 2.1, we identify $\lambda = 0$ with the reference point $\boldsymbol{r}_0$, corresponding to the beginning of the congruence, and we identify the *fixed, finite* value $\lambda = L$ with $\boldsymbol{r} = \boldsymbol{r}\left(L, \boldsymbol{r}_0\right)$, corresponding to the end of the congruence. In general, we take the reference point $\boldsymbol{r}_0$ and end point $\boldsymbol{r}\left(L, \boldsymbol{r}_0\right)$ on the system boundary[4]. From this perspective, *each particular field line solution with $L > 0$ provides a unique connectivity map between disjoint points on the system boundary, and the spatial propagator quantifies the local geometric organization in this connectivity map.*

At $\boldsymbol{r}_0$, the boundary surface $z = -L_z$ has a unit normal $\hat{\boldsymbol{n}}\left(\boldsymbol{r}_0\right) = \boldsymbol{e}_z$. We may construct two orthogonal reference shift vectors $\{\boldsymbol{h}_1, \boldsymbol{h}_2\}$ tangent to the $z = -L_z$ boundary plane; that is, both $\{\boldsymbol{h}_1, \boldsymbol{h}_2\}$ satisfy a tangency constraint, $\boldsymbol{h}_\alpha \cdot \hat{\boldsymbol{n}}\left(\boldsymbol{r}_0\right) = 0$ for each $\alpha = 1, 2$. In this case, without loss of generality, we may choose the $\{\boldsymbol{h}_1, \boldsymbol{h}_2\}$ proportional to the basis vectors $\{\boldsymbol{e}_x, \boldsymbol{e}_y\}$. Written with respect to the global $\{\boldsymbol{e}_x, \boldsymbol{e}_y, \boldsymbol{e}_z\}$ basis, the reference shift vectors are

$$\boldsymbol{h}_1 \;=\; \left(\,|\boldsymbol{h}_1|\,\right)^x \boldsymbol{e}_x,$$

---

[4]In solar and coronal physics applications, the system boundary is typically taken to be the photosphere-photosphere, or photosphere-source surface ansatz.
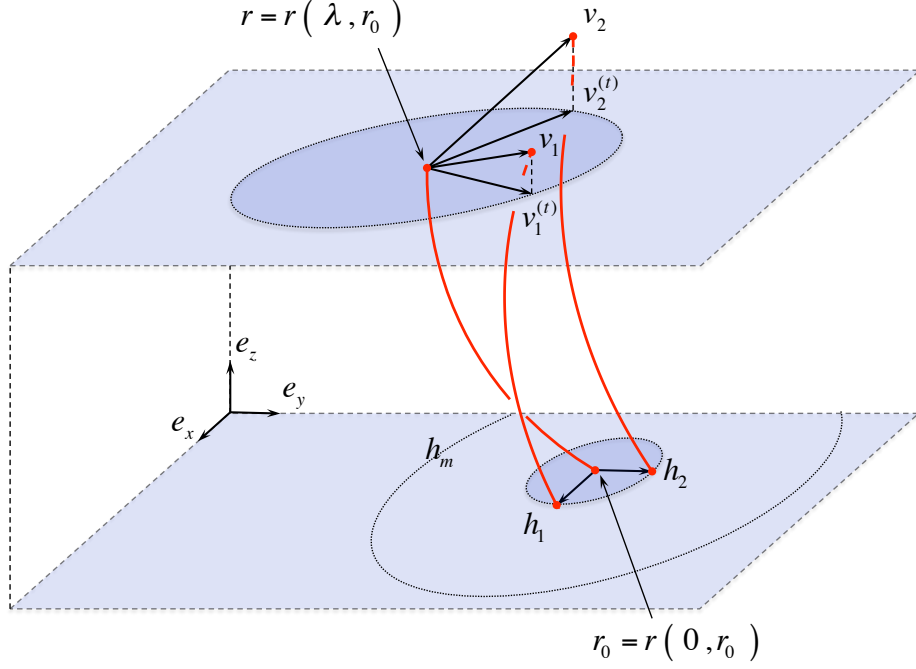
Figure 6. Illustration of the QSL geometry. Simple example with top, resp. bottom, boundaries at $z = \pm L_z$. An initial circle defined via $\{\boldsymbol{h}_1, \boldsymbol{h}_2\}$ deforms into an ellipsoid defined via the projections $\{\boldsymbol{v}_1^{(t)}, \boldsymbol{v}_2^{(t)}\}$ of the propagated vectors $\{\boldsymbol{v}_1, \boldsymbol{v}_2\}$ on to the plane $z = L_z$.

$$\boldsymbol{h}_2 \;=\; (\, |\boldsymbol{h}_2| \,)^y \, \boldsymbol{e}_y. \tag{50}$$

Moreover, the components of each reference shift vector $\boldsymbol{h}_\alpha$ are subject to the characteristic scale constraint; for $\alpha = 1, 2$,

$$|\boldsymbol{h}_\alpha| \;=\; \left(\sum_i (\, \boldsymbol{h}_\alpha \,)^i (\, \boldsymbol{h}_\alpha \,)^i \right)^{1/2} << h_m. \tag{51}$$

where h_m is defined in Appendix A.

By Equation (12), these reference shift vectors $\{\boldsymbol{h}_1, \boldsymbol{h}_2\}$ are propagated along the congruence to the target foot point $\boldsymbol{r}(L, \boldsymbol{r}_0)$. The propagated vectors at $\lambda = L$ are also written with respect to the global $\{\boldsymbol{e}_x, \boldsymbol{e}_y, \boldsymbol{e}_z\}$ basis,

$$
\begin{aligned}
\boldsymbol{v}_1(L, \boldsymbol{r}_0) &= \sum_i (\, \mathbf{F}|_{L, \boldsymbol{r}_0} \,)^i{}_x (\, |\boldsymbol{h}_1| \,)^x \, \boldsymbol{e}_i, \\
\boldsymbol{v}_2(L, \boldsymbol{r}_0) &= \sum_i (\, \mathbf{F}|_{L, \boldsymbol{r}_0} \,)^i{}_y (\, |\boldsymbol{h}_2| \,)^y \, \boldsymbol{e}_i.
\end{aligned}
\tag{52}
$$

We note, since by assumption the vector field $\boldsymbol{B}(\boldsymbol{r})$ is everywhere smooth, the spatial propagator $\mathbf{F}(\lambda, \boldsymbol{r}_0)$ is non-singular for all λ, then all linearly independent $\{\boldsymbol{h}_1, \boldsymbol{h}_2\}$ are mapped to linearly independent $\{\boldsymbol{v}_1(L, \boldsymbol{r}_0), \boldsymbol{v}_2(L, \boldsymbol{r}_0)\}$.

Furthermore, while we have the freedom to chose the reference shift vectors $\boldsymbol{h}_\alpha$ tangent to the boundary surface at the launch footpoint $\boldsymbol{r}_0$, the propagated vectors $\boldsymbol{v}_\alpha(L, \boldsymbol{r}_0)$ at the target footpoint $\boldsymbol{r}(L, \boldsymbol{r}_0)$ are, in general, *not* tangent to their respective boundary surface. However, we may project the $\boldsymbol{v}_\alpha(L, \boldsymbol{r}_0)$ onto the tangent boundary plane (see Figure 6); that is,

$$\boldsymbol{v}_\alpha^{(t)}(L, \boldsymbol{r}_0) \;=\; (\; \mathbf{I} - \hat{\boldsymbol{n}}(\boldsymbol{r}) \otimes \hat{\boldsymbol{n}}(\boldsymbol{r})\;) \cdot \boldsymbol{v}_\alpha(L, \boldsymbol{r}_0), \tag{53}$$

with $r = \boldsymbol{r}(L, \boldsymbol{r}_0)$ at the target footpoint. The superscript (t) denotes projection tangent to the boundary. In our simple example, at the target footpoint, $\boldsymbol{r} = \boldsymbol{r}(L, \boldsymbol{r}_0)$, the $\hat{\boldsymbol{n}}(\boldsymbol{r}) = -\boldsymbol{e}_z$ and Equation (53) yields,

$$
\begin{aligned}
\boldsymbol{v}_1^{(t)}(L, \boldsymbol{r}_0) &= (\; \mathbf{F}|_{L,\boldsymbol{r}_0}\;)^x{}_x\,(\;|\boldsymbol{h}_1|\;)^x\,\boldsymbol{e}_x + (\;\mathbf{F}|_{L,\boldsymbol{r}_0}\;)^y{}_x\,(\;|\boldsymbol{h}_1|\;)^x\,\boldsymbol{e}_y \\
\boldsymbol{v}_2^{(t)}(L, \boldsymbol{r}_0) &= (\;\mathbf{F}|_{L,\boldsymbol{r}_0}\;)^x{}_y\,(\;|\boldsymbol{h}_2|\;)^y\,\boldsymbol{e}_x + (\;\mathbf{F}|_{L,\boldsymbol{r}_0}\;)^y{}_y\,(\;|\boldsymbol{h}_2|\;)^y\,\boldsymbol{e}_y.
\end{aligned} \tag{54}
$$

We remark, the above construction/projection procedure is valid for any surface with normal $\hat{\boldsymbol{n}}(\boldsymbol{r})$ on the system boundary.

The local properties of the mapping of vectors $\boldsymbol{h}_\alpha$ tangent to the boundary plane at $\boldsymbol{r}_0$, into vectors $\boldsymbol{v}_\alpha^{(t)}(L, \boldsymbol{r}_0)$ tangent to the boundary plane at $\boldsymbol{r} = \boldsymbol{r}(L, \boldsymbol{r}_0)$ are described by the 2×2 matrix $\mathcal{D}$; the components of which are,

$$(\;\mathcal{D}\;)^i{}_j \;:=\; \frac{\left(\;\boldsymbol{v}_\alpha^{(t)}|_{L,\boldsymbol{r}_0}\;\right)^i}{(\;\boldsymbol{h}_\alpha\;)^j} = \begin{pmatrix} (\;\mathbf{F}|_{L,\boldsymbol{r}_0}\;)^x{}_x & (\;\mathbf{F}|_{L,\boldsymbol{r}_0}\;)^y{}_x \\[2mm] (\;\mathbf{F}|_{L,\boldsymbol{r}_0}\;)^x{}_y & (\;\mathbf{F}|_{L,\boldsymbol{r}_0}\;)^y{}_y \end{pmatrix}. \tag{55}$$

The matrix $\mathcal{D}$ is the submatrix of $\mathbf{F}(L, \boldsymbol{r}_0)$ obtained by removing the column corresponding to the coordinate direction parallel to the launch surface normal, and row corresponding to the coordinate direction parallel to the target surface normal; in this example, remove the column $(\;\mathbf{F}|_{L,\boldsymbol{r}_0}\;)^z{}_j$ and remove the row $(\;\mathbf{F}|_{L,\boldsymbol{r}_0}\;)^i{}_z$. This principle is the same for general curvilinear coordinate systems at the boundaries. More generally, boundary surface unit normals may not be parallel to coordinate directions at all positions on the boundary surface. Hence the tensorial nature of the Spatial Propagator allows one to simply rotate the proper components of the 3×3 matrix into coordinates parallel to the surface normals at the point on appropriate boundaries, and then remove the appropriate rows/columns to construct the proper 2×2 sub-matrix; we leave such analysis for future work.

The field lines define a map from h-coordinates with origin at $\boldsymbol{r}_0$, to $v^{(t)}$-coordinates with origin at $\boldsymbol{r} = \boldsymbol{r}(L, \boldsymbol{r}_0)$. By Equations (16) and (17), the basis vectors $\boldsymbol{h}_\alpha$ are propagated, via Lie transport (Scott et al., 2017), from $\boldsymbol{r}_0$ to $\boldsymbol{r} = \boldsymbol{r}(L, \boldsymbol{r}_0)$. The matrix $\mathcal{D}$ may be interpreted as the Jacobian of this map, given by the corresponding components of the matrix representation of the spatial propagator $(\;\mathbf{F}|_{L,\boldsymbol{r}_0}\;)^i{}_j$. The squashing factor, Q, may be immediately constructed; in the notation of Titov et al. (2002),

$$Q = \frac{N^2}{\Delta}, \tag{56}$$

where the Norm, (N; Démoulin et al., 1996) is given by

$$N^2 \; = \; \left(\left(\; \mathbf{F}|_{L,\boldsymbol{r}_0} \;\right){}^{x}{}_{x}\right)^2 + \left(\left(\; \mathbf{F}|_{L,\boldsymbol{r}_0} \;\right){}^{y}{}_{y}\right)^2 + \left(\left(\; \mathbf{F}|_{L,\boldsymbol{r}_0} \;\right){}^{x}{}_{y}\right)^2 + \left(\left(\; \mathbf{F}|_{L,\boldsymbol{r}_0} \;\right){}^{y}{}_{x}\right)^2, \tag{57}$$

and Δ is the determinant of the Jacobian matrix $\mathcal{D}$,

$$\Delta \; = \; \left(\; \mathbf{F}|_{L,\boldsymbol{r}_0} \;\right){}^{x}{}_{x} \left(\; \mathbf{F}|_{L,\boldsymbol{r}_0} \;\right){}^{y}{}_{y} - \left(\; \mathbf{F}|_{L,\boldsymbol{r}_0} \;\right){}^{x}{}_{y} \left(\; \mathbf{F}|_{L,\boldsymbol{r}_0} \;\right){}^{y}{}_{x}. \tag{58}$$

More generally, Equation (58) is the minor of the submatrix corresponding to the $\left(\; \mathbf{F}|_{L,\boldsymbol{r}_0} \;\right){}^{i}{}_{j}$ matrix component, where the i-index corresponds to the coordinate direction parallel to the launch surface normal, and the j-index corresponds to the coordinate direction parallel to the target surface normal.

Moreover, the eigenvalues $\{d_1, d_2\}$ of the 2×2 Jacobian matrix $\mathcal{D}$, given by the roots of the characteristic equation,

$$\det \left(\; \mathcal{D} - d\, \mathbf{I} \;\right) \; = \; 0,$$

are related to the Q-value via

$$\frac{|d_1|}{|d_2|} \; = \; \frac{Q}{2} + \left(\; \left(\frac{Q}{2}\right)^2 - 1 \;\right)^{1/2}, \tag{59}$$

which, after some algebra, reduces to

$$Q = \frac{d_1}{d_2} + \frac{d_2}{d_1}. \tag{60}$$

We remark, fixing the boundary surfaces under line tying condition does not imply a fixed Spatial Propagator, only the proper sub-matrices and their combinatorics forming the squashing factor, Q, are preserved.

The Q-Map (Titov, 2007), identifies the separatrix and QSL field structures. However, on their own, these regions offer only the *possible* current sheet formation sites in the field structure. Whether or not electromagnetic stresses accumulate resulting in subsequent current sheet formation, depends on the details of energization and stress injection; e.g., separatrix and QSL structures undergoing rigid body motion will not develop a current sheet (Aulanier et al., 2005, 2010; Janvier et al., 2014); whereas more general motions, such as shearing or twisting motions, will develop a current sheet unstable to reconnection (Aulanier et al., 2006; Effenberger et al., 2011; Janvier et al., 2013).

4. Conclusion and Future Applications

In this paper we introduce a generalized field line connectivity phase space associated to the vector magnetic field in which the geometric and topological features of the system are made explicit. The fundamental assumption is that the

vector magnetic field is *a-priori* smooth everywhere. The basic elements, Equations (19), are the field line and its linearized variation, the spatial propagator. Equations (2) and (16), with initial conditions (3) and (17), provide a direct formulation of these phase space elements in terms of the vector magnetic field and its spatial derivatives. Furthermore, the field line and spatial propagator are constructed with respect to general curvilinear coordinates and the equivalence class of general affine parameterizations.

The geometric interpretation is that the spatial propagator characterizes the organization of the local bundle of field lines. Since the vector field is everywhere smooth, so too are the field line and spatial propagator solutions smooth and unique. The geometric organization of the local bundle is completely equivalent to a kinematic description of a volume centered on the particular field line solution and undergoing deformation by transport along the field. This deformation kinematics is characterized by volumetric dilation, anisotropic stretch, and rotation. The volumetric dilation (expansion/compression) is completely described by the determinant of the spatial propagator, Equation (30). For the vector magnetic field, the determinant of the spatial propagator is a topological invariant everywhere equal to one, Equation (34). This topological invariant reflects the divergence-free condition. The anisotropic stretch and rotation kinematics are described by the singular values and singular vectors of the spatial propagator. The singular values, Equation (37), characterize the general anisotropic stretch of the congruence volume. The congruence rotation is a simple rigid body rotation kinematics between the orthonormal principle direction bases, Equation (43), from the reference volume Ω_0 to the propagated volume Ω_λ.

Extreme singular values identify QSLs within the system; true separatrix surfaces, respectively separator lines, within the system are identified in the limiting cases of one, respectively two, zero singular values. Moreover, the Q-factor is simply constructed from analysis of the particular submatrix of the spatial propagator obtained by removing the column corresponding to the coordinate direction parallel to the launch surface normal, and row corresponding to the coordinate direction parallel to the target surface normal.

This connectivity phase space framework opens up extensive directions in geometric and topological analysis of vector magnetic fields. For example, in future work we will relax the a-priori smooth vector magnetic field assumption in order to analyze both existing, as well as the formation of, singular structures such as current sheets. Moreover, magnetic helicity may be decomposed into twist and writhe components (Moffatt & Ricca, 1992); in future efforts we will show that, accounting for relative shearing of the volume, twist helicity may be described with the congruence rotation, while the writhe helicity is related to the embedding of the field line trajectory and propagation of the reference shift vector in 3D space.

In the present work the field line bundle and spatial propagator are presented and analyzed from a purely geometric perspective; the analogy made is to a purely kinematical description of the system. Since the field lines are curves (i.e., *spatial positions*) in three-dimensional space whose tangent vector is everywhere parallel to the magnetic field vector, evolutionary dynamics (ideal or otherwise) of the field line bundle are often described by imposing the frozen-in condition

(e.g., infinite plasma conductivity) somewhere within the system domain (typically at the system boundary) which then allows one to follow the dynamics of a parcel of plasma to which the field line is connected. In these systems, the difference between ideal motions and actual motion of the field is attributed to resistive slipping; this is the origin of "slip-running reconnection" and other resistive slip phenomenology. In follow-up analysis, we use this formalism to describe the dynamics of a field line bundle and associated the spatial propagator without reference to plasma conductivity, or material parcels, but rather with respect to pure electric and magnetic fields; such a description necessarily requires a treatment of the full four-dimensional electromagnetic field tensor.

In particular, the magnetic field generalizes to the anti-symmetric, dual electromagnetic tensor field, $*\mathcal{F}^{\mu\nu}$ ($t, \boldsymbol{x}$) (see e.g., Jackson, 1999, §11.9). The field line bundle generalizes to a 4-vector flow field ϕ^{μ} ($t, \boldsymbol{x}$), where the spatial components of which are identified with the current canonical notion of a field line. And the Propagator generalizes to a 2nd-order tensor field, $F^{\mu}{}_{\nu}$ ($t, \boldsymbol{x}$); the spatial components of which are identified with the Spatial Propagator. We will show that expanding these generalizations into their explicit time and spatial components recovers the definition of a magnetic field line as a *spatial-constraint* equation,

$$(\boldsymbol{B} \cdot \nabla) \phi^i = B^i, \tag{61}$$

and *time-dynamic* equations for the field line components evaluated at each ($t, \boldsymbol{x}$),

$$\frac{B^2}{4\pi} \frac{\partial \phi^i}{\partial t} + (\boldsymbol{S} \cdot \nabla) \phi^i = S^i. \tag{62}$$

where $\boldsymbol{S}$ is the Poynting vector (Jackson, 1999, p. 608-610).

Finally, this framework allows for the analysis of extrinsic thermodynamic properties, such as the total mass or total total magnetic energy, of the field line bundle. In particular, we derive an analogous First Law of Thermodynamics applied to the pure magnetic congruence geometry,

$$\Delta E \ (L, 0; \Omega_0) = E (L, \Omega_0) - E (0, \Omega_0)$$
$$= \int_0^L \int_{\Omega_0} \left(\mathrm{Tr} (\, \mathbf{T} \cdot (\nabla \boldsymbol{B}) \,) + \rho \, \boldsymbol{E} \cdot \boldsymbol{B} + \frac{1}{c^2} \, \boldsymbol{E} \cdot (\, \nabla \times \boldsymbol{S} \,) \right) \mathrm{d}^3\boldsymbol{x} \, \mathrm{d}\lambda, \tag{63}$$

where $\boldsymbol{E}$ and $\boldsymbol{B}$ are the electric and magnetic fields, $\mathbf{T}$ is the the electromagnetic stress tensor, ρ is the net charge density, and $\boldsymbol{S}$ is the Poynting vector (Jackson, 1999, p. 608-610); all quantities are evaluated along the field line $\boldsymbol{r} = \boldsymbol{r} (\lambda, \boldsymbol{r}_0)$. Equation (63) is the total electromagnetic energy of a congruence formulated in terms analogous to mechanical work and energy generation. We will derive Equation (63) and explore applications to coronal phenomenology (e.g., coronal heating, active region stability, flares, and CME initiation) in future work.

Appendix

A. Characteristic Scale h_m of the Spatial Propagator

In this appendix, we derive the local characteristic scale h_m over which the spatial propagator $\mathbf{F}(\lambda, \boldsymbol{r}_0)$ describes the relative behavior of field lines within a congruence. The family of integral curve solutions $\boldsymbol{r}(\lambda, \boldsymbol{r}_0)$ to the system (2) and (3) are written in components with respect to a generally valid global basis $\boldsymbol{e}_i$ (see Appendix B.1),

$$\boldsymbol{r}(\lambda, \boldsymbol{r}_0) = \sum_i (\, \boldsymbol{r}|_{\lambda,\boldsymbol{r}_0}\,)^i\, \boldsymbol{e}_i \tag{64}$$

where the component functions, $(\, \boldsymbol{r}|_{\lambda,\boldsymbol{r}_0}\,)^i$, are smooth functions of the connectivity parameter λ, and reference condition coordinates $\boldsymbol{r}_0$.

Consider two spatially neighboring field lines within the congruence, $\boldsymbol{r}(\lambda, \boldsymbol{r}_0)$ and $\boldsymbol{r}(\lambda, \boldsymbol{r}_0 + \boldsymbol{h})$. We may relate the neighboring field lines via Taylor expansion of the component functions,

$$
\begin{aligned}
(\, \boldsymbol{r}|_{\lambda,\boldsymbol{r}_0+\boldsymbol{h}}\,)^i &- (\, \boldsymbol{r}|_{\lambda,\boldsymbol{r}_0}\,)^i \\
&= \sum_j (\, \mathbf{F}|_{\lambda,\boldsymbol{r}_0}\,)^i{}_j\, h^j + \frac{1}{2} \sum_{j,k} (\, \mathbf{M}|_{\lambda,\boldsymbol{r}_0}\,)^i{}_{jk}\, h^j h^k + O\left(|\boldsymbol{h}|^3\right).
\end{aligned}
\tag{65}
$$

In the most general case, the congruence solution $\boldsymbol{r}(\lambda, \boldsymbol{r}_0)$ is a non-linear function of the reference point $\boldsymbol{r}_0$. In this case, the components (at least one) of the second-order variation are non-trivial; i.e., $(\, \mathbf{M}|_{\lambda,\boldsymbol{r}_0}\,)^i{}_{jk} \neq 0$. Hence, we may define the characteristic scale h_m of the spatial propagator $\mathbf{F}(\lambda, \boldsymbol{r}_0)$ by considering the relative size of the first and second order variational terms.

$$
\begin{aligned}
\left| (\, \boldsymbol{r}|_{\lambda,\boldsymbol{r}_0+\boldsymbol{h}}\,)^i \right. &\left. - (\, \boldsymbol{r}|_{\lambda,\boldsymbol{r}_0}\,)^i \right| \\
&= \left| \sum_j (\, \mathbf{F}|_{\lambda,\boldsymbol{r}_0}\,)^i{}_j\, h^j + \frac{1}{2} \sum_{j,k} (\, \mathbf{M}|_{\lambda,\boldsymbol{r}_0}\,)^i{}_{jk}\, h^j h^k + O\left(|\boldsymbol{h}|^3\right) \right|
\end{aligned}
$$

$$
\leq \left| \sum_j (\mathbf{F}|_{\lambda, \boldsymbol{r}_0})^i{}_j \, h^j \right| + \left| \frac{1}{2} \sum_{j,k} (\mathbf{M}|_{\lambda, \boldsymbol{r}_0})^i{}_{jk} \, h^j h^k \right| + O\left(|\boldsymbol{h}|^3\right)
$$

$$
\leq \left| \sum_j (\mathbf{F}|_{\lambda, \boldsymbol{r}_0})^i{}_j \right| |\boldsymbol{h}| + \frac{1}{2} \left| \sum_{j,k} (\mathbf{M}|_{\lambda, \boldsymbol{r}_0})^i{}_{jk} \right| |\boldsymbol{h}|^2 + O\left(|\boldsymbol{h}|^3\right).
$$

(66)

Since the vector field $\boldsymbol{B}(\boldsymbol{r})$ is assumed smooth everywhere, it may be shown the $L_{1,2}$ norm of the first- and second-order variation matrices $||\mathbf{F}||$ and $||\mathbf{M}||$ are non-singular; that is, there exists a finite $F, M \in \mathbb{R}$ such that

$$
F := ||\mathbf{F}|_{\boldsymbol{r}_0}|| = \max_\lambda \left(\sum_i \left(\sum_j (\mathbf{F}|_{\lambda, \boldsymbol{r}_0})^i{}_j \right)^2 \right)^{1/2} , \qquad (67)
$$

$$
M := ||\mathbf{M}|_{\boldsymbol{r}_0}|| = \max_\lambda \left(\sum_i \left(\sum_{j,k} (\mathbf{M}|_{\lambda, \boldsymbol{r}_0})^i{}_{jk} \right)^2 \right)^{1/2} . \qquad (68)
$$

Hence, (66) becomes

$$
\left| (\boldsymbol{r}|_{\lambda, \boldsymbol{r}_0 + \boldsymbol{h}})^i - (\boldsymbol{r}|_{\lambda, \boldsymbol{r}_0})^i \right| \leq F \, |\boldsymbol{h}| + \frac{M}{2} \, |\boldsymbol{h}|^2 + O\left(|\boldsymbol{h}|^3\right)
$$

$$
\leq F \, |\boldsymbol{h}| \left(1 + \frac{M}{2F} \, |\boldsymbol{h}| + O\left(|\boldsymbol{h}|^2\right) \right)
$$

$$
\leq F \, |\boldsymbol{h}| \left(1 + \frac{|\boldsymbol{h}|}{h_m} + O\left(|\boldsymbol{h}|^2\right) \right). \qquad (69)
$$

Where we defined the characteristic scale $h_m := 2F/M$; that is, the characteristic scale is the minimum scale such that the linear term is at least of the same magnitude as the second order term. Then, for all $|\boldsymbol{h}| \ll h_m$, the higher-order terms of Equation (69) are all negligible relative to the first-order term, and the first-order variation $\mathbf{F}(\lambda, \boldsymbol{r}_0)$ describes the relative behavior of the congruence.

In the special case, that the congruence solution $\boldsymbol{r}(\lambda, \boldsymbol{r}_0)$ is linear in reference point $\boldsymbol{r}_0$, then all components of $(\mathbf{M}|_{\lambda, \boldsymbol{r}_0})^i{}_{jk} = 0$, and all higher-order derivatives vanish, and $h_m \to \infty$. Hence, for all $\boldsymbol{h} \in \mathbb{R}^3$,

$$
(\boldsymbol{r}|_{\lambda, \boldsymbol{r}_0 + \boldsymbol{h}})^i - (\boldsymbol{r}|_{\lambda, \boldsymbol{r}_0})^i = \sum_j (\mathbf{F}|_{\lambda, \boldsymbol{r}_0})^i{}_j \, h^j \qquad (70)
$$

Furthermore, for completeness, in cases of high symmetry, the higher-order variations may vanish through some finite order n. In such examples, the characteristic scale is defined as $h_m := \left(\dfrac{(n+1)! \, F}{M^{(n+1)}} \right)^{1/n}$ with $n \geq 2$, where $M^{(n+1)}$ is the $L_{1,2}$ norm of lowest-order non-zero variation matrix. We do not pursue such cases here.

An extremely popular approach to computational solar, and space plasma physics is the linear interpolation methodologies employed in numerical algorithms for the computation of vector field components between grid points (see e.g., Tassev & Savcheva, 2017). Such approaches simply shifts the problem of investigating small scale dynamics from the physical vector magnetic field on to finer and more complex numerical grid resolutions. Depending on the size of h_m relative to the characteristic scales of the system, this may be a fundamental limitation as an accurate representation of the vector field structure. The formalism presented here is a fundamentally different approach in which the investigative burden remains on the physical quantities, as opposed to simply increasing the computational expense to handle finer and finer mesh structure.

B. Matrix Representation of the Covariant Differential of a Vector Field with Respect to General Basis

In this appendix, we briefly review some aspects of canonical differential geometry (e.g., general coordinate charts, basis and dual basis vectors, and the differential operator ∇). In particular, we construct the (3×3) matrix representation of the covariant differential $\nabla \boldsymbol{B}\,(\boldsymbol{r})$ with respect to general, local curvilinear bases. The term *covariant* is standard nomenclature; in this context, meaning the object transforms as a tensor under general coordinate transformations. We construct the matrix representation of the covariant differential $\nabla \boldsymbol{B}\,(\boldsymbol{r})$ with respect to a general coordinate chart (Appendix B.1), followed by the respective applications to the spherical-polar curvilinear coordinate basis (Appendix B.2), and the spherical-polar orthonormal basis (Appendix B.3) in common use by the solar and space physics community (see e.g., Tassev & Savcheva, 2017).

We note, this appendix is not intended to be a full exposition of differential geometry. We describe only those aspects necessary and sufficient for the construction of the covariant differential of the vector field in curvilinear coordinates; see Kobayashi & Nomizu (1963) for a full axiomatic approach.

B.1. General Construction of the Covariant Differential of a Vector Field

B.1.1. General Curvilinear Coordinates, Basis and Dual Basis Vectors

Let $M \subseteq \mathbb{R}^3$ be a subset of three dimensional space. Consider a general curvilinear coordinate chart (M, q) such that the position of each point $p \in M$ is described by smooth coordinate functions $q : M \to \mathbb{R}^3$,

$$\boldsymbol{r}\,(p) \; = \; \{\; q^1\,(p)\,, q^2\,(p)\,, q^3\,(p)\;\}. \tag{71}$$

For ease of notation, we drop the formal dependence on the point $p \in M$, labeling it with only the coordinates q^i.

The coordinate chart (M, q) admits a natural set of coordinate basis vectors, $\{\boldsymbol{q}_1, \boldsymbol{q}_2, \boldsymbol{q}_3\}$. The (not necessarily orthonormal) basis vector $\boldsymbol{q}_i$ is the unique

element of the tangent bundle that acts on the (smooth) position vector by taking its derivative with respect to the coordinate q^i,

$$\boldsymbol{q}_i := \frac{\partial \boldsymbol{r}}{\partial q^i}. \tag{72}$$

The coordinate basis vectors, $\{\boldsymbol{q}_1, \boldsymbol{q}_2, \boldsymbol{q}_3\}$, are often written explicitly with respect to Cartesian basis set $\{\boldsymbol{e}_x, \boldsymbol{e}_y, \boldsymbol{e}_z\}$. Assume the general curvilinear coordinates are smoothly related to Cartesian coordinates; that is, there exist smooth coordinate transformation functions,

$$x^j = x^j \left(q^i \right), \tag{73}$$

such that the position vector, (71), has components written with respect to the $\{\boldsymbol{e}_x, \boldsymbol{e}_y, \boldsymbol{e}_z\}$ basis,

$$\boldsymbol{r} \; = \; \sum_j \, x^j \left(q^i \right) \boldsymbol{e}_j. \tag{74}$$

Since the Cartesian basis vectors $\boldsymbol{e}_i$ are independent of position, definition (72) leads to each basis vector $\boldsymbol{q}_i$ expanded in components with respect to the standard Cartesian basis,

$$\boldsymbol{q}_i \; = \; \sum_j \, \frac{\partial x^j}{\partial q^i} \, \boldsymbol{e}_j. \tag{75}$$

In general, the components of the Jacobian are functions of position, $\boldsymbol{q}_i = \boldsymbol{q}_i \left(q^j \right)$.

Moreover, for a given basis $\boldsymbol{q}_i$ there exists a unique dual basis $\boldsymbol{q}^i$ defined as those linear functionals that satisfy

$$\boldsymbol{q}^i \cdot \boldsymbol{q}_j := \delta^i{}_j. \tag{76}$$

(See e.g., Kobayashi & Nomizu, 1963, p. 4-6 for details). Since the coordinate transformation functions, (73), are assumed smooth, that is the Jacobian is locally invertible, the inverse coordinate transformation functions exist. Hence, similar to Equation (75), the dual basis $\boldsymbol{q}^i$ may be written in components with respect to the standard Cartesian basis,

$$\boldsymbol{q}^i \; = \; \sum_j \, \frac{\partial q^i}{\partial x^j} \, \boldsymbol{e}_j. \tag{77}$$

In general, the components of the inverse Jacobian are functions of position, $\boldsymbol{q}^i = \boldsymbol{q}^i \left(q^j \right)$.

B.1.2. The Metric and the Inner-Product

The standard inner-product between two Cartesian vectors $\boldsymbol{u}$ and $\boldsymbol{u}'$ is a binary operation defined by $\boldsymbol{u} \cdot \boldsymbol{u}' = \sum_i \, u^i \, u'^i$, where u^i and u'^i are the components

with respect to the standard Cartesian basis. Moreover, the inner-product is symmetric $\boldsymbol{u} \cdot \boldsymbol{u}' = \boldsymbol{u}' \cdot \boldsymbol{u}$, non-degenerate $\boldsymbol{u} \cdot \boldsymbol{u}' = \boldsymbol{u} \cdot \boldsymbol{u}''$ if and only if $\boldsymbol{u}' = \boldsymbol{u}''$, and positive-definite $\boldsymbol{u} \cdot \boldsymbol{u} \geq 0$ where the equality holds if and only if $\boldsymbol{u} = 0$,

More generally, the inner-product operation between two vectors with components given with respect to a general (curvilinear) basis is defined by a bilinear form $\mathbf{g}$ known as the metric (see e.g., Kobayashi & Nomizu, 1963, p. 24), $\mathbf{g}(\boldsymbol{u}, \boldsymbol{u}') := \boldsymbol{u} \cdot \boldsymbol{u}'$. The metric $\mathbf{g}$ is symmetric, $\mathbf{g}(\boldsymbol{u}, \boldsymbol{u}') = \mathbf{g}(\boldsymbol{u}', \boldsymbol{u})$, non-degenerate, $\mathbf{g}(\boldsymbol{u}, \boldsymbol{u}') = \mathbf{g}(\boldsymbol{u}, \boldsymbol{u}'')$ if and only if $\boldsymbol{u}' = \boldsymbol{u}''$, and positive-definite, $\mathbf{g}(\boldsymbol{u}, \boldsymbol{u}) \geq 0$ where the equality holds if and only if $\boldsymbol{u} = 0$.

Any vector $\boldsymbol{u}$ may be represented as a linear combination of smooth components with respect to the basis $\boldsymbol{q}_i$,

$$\boldsymbol{u} = \sum_i u^i \, \boldsymbol{q}_i. \tag{78}$$

Hence, the inner-product between two vectors with components given with respect to the basis $\boldsymbol{q}_i$ is

$$\boldsymbol{u} \cdot \boldsymbol{u}' = \mathbf{g}(\boldsymbol{u}, \boldsymbol{u}') = \sum_{i,j} u^i \, u'^j \, \mathbf{g}(\boldsymbol{q}_i, \boldsymbol{q}_j) = \sum_{i,j} u^i \, u'^j \, g_{ij}. \tag{79}$$

The scalar values, $g_{ij} = \mathbf{g}(\boldsymbol{q}_i, \boldsymbol{q}_j)$, are simply the inner-product between basis vectors $\boldsymbol{q}_i$. The g_{ij} may be calculated using Equation (75),

$$g_{ij} = \boldsymbol{q}_i \cdot \boldsymbol{q}_j = \sum_{k,l} \frac{\partial x^k}{\partial q^i} \frac{\partial x^l}{\partial q^j} (\, \boldsymbol{e}_k \cdot \boldsymbol{e}_l \,) = \sum_{k,l} \frac{\partial x^k}{\partial q^i} \frac{\partial x^l}{\partial q^j} \, \delta_{kl} = \sum_k \frac{\partial x^k}{\partial q^i} \frac{\partial x^k}{\partial q^j}. \tag{80}$$

By similar arguments, we may construct (inverse) scalars, $g^{ij} = \mathbf{g}(\boldsymbol{q}^i, \boldsymbol{q}^j)$, using Equation (77),

$$g^{ij} = \boldsymbol{q}^i \cdot \boldsymbol{q}^j = \sum_{k,l} \frac{\partial q^i}{\partial x^k} \frac{\partial q^j}{\partial x^l} (\, \boldsymbol{e}_k \cdot \boldsymbol{e}_l \,) = \sum_{k,l} \frac{\partial q^i}{\partial x^k} \frac{\partial q^j}{\partial x^l} \, \delta_{kl} = \sum_k \frac{\partial q^i}{\partial x^k} \frac{\partial q^j}{\partial x^k}. \tag{81}$$

In general, the scalars $g_{ij} = g_{ij}(q^k)$, and $g^{ij} = g^{ij}(q^k)$, are functions of position. Furthermore, Equations (80) and (81) satisfy

$$\sum_k g_{ik} \, g^{kj} = \sum_k g^{ik} \, g_{kj} = \delta^i{}_j. \tag{82}$$

The scalars g_{ij} and g^{ij} may be represented as 3×3 invertible matrices,

$$\mathbf{g} = \sum_{i,j} g_{ij} \, \boldsymbol{q}^i \otimes \boldsymbol{q}^j, \quad \text{and} \quad \mathbf{g}^{-1} = \sum_{i,j} g^{ij} \, \boldsymbol{q}_i \otimes \boldsymbol{q}_j. \tag{83}$$

We remark, it is conventional to define the g_{ij} to be the components of the metric $\mathbf{g}$, and the g^{ij} the components of the inverse metric $\mathbf{g}^{-1}$.

By the non-degeneracy assumption, Equations (75), (77), (80), and (81), the metric and inverse metric provide a natural isomorphism between the $\boldsymbol{q}_i$ and $\boldsymbol{q}^i$. By Equations (81) and (75)

$$
\begin{aligned}
\sum_j g^{ij} \, \boldsymbol{q}_j &= \sum_j \left(\sum_k \frac{\partial q^i}{\partial x^k} \frac{\partial q^j}{\partial x^k} \right) \left(\sum_l \frac{\partial x^l}{\partial q^j} \, \boldsymbol{e}_l \right) \\
&= \sum_{j,k,l} \frac{\partial q^i}{\partial x^k} \frac{\partial q^j}{\partial x^k} \frac{\partial x^l}{\partial q^j} \, \boldsymbol{e}_l \\
&= \sum_{k,l} \frac{\partial q^i}{\partial x^k} \, \delta_k{}^l \, \boldsymbol{e}_l \\
&= \sum_k \frac{\partial q^i}{\partial x^k} \, \boldsymbol{e}_k \\
&= \boldsymbol{q}^i,
\end{aligned}
\tag{84}
$$

where, in the last step we used definition (77). A similar calculation with Equations (80), (77), and (75) yields,

$$
\sum_j g_{ij} \, \boldsymbol{q}^j = \boldsymbol{q}_i.
\tag{85}
$$

B.1.3. Curvilinear Coordinates and Orthonormal Bases

On the other hand, one may always construct an orthonormal basis $\hat{\boldsymbol{q}}_i$, respectively dual $\hat{\boldsymbol{q}}^i$, from linear combinations of the curvilinear basis $\boldsymbol{q}_i$, respectively dual $\boldsymbol{q}^i$, bases,

$$
\hat{\boldsymbol{q}}_i := \sum_j M_i{}^j \, \boldsymbol{q}_j \quad \text{and} \quad \hat{\boldsymbol{q}}^i := \sum_j N^i{}_j \, \boldsymbol{q}^j.
\tag{86}
$$

The components of the transformation matrices are smooth functions of the coordinates, $M_i{}^j = M_i{}^j \left(q^k \right)$, respectively $N^i{}_j \left(q^k \right)$. In particular, the matrix components $M_i{}^j$ and $N^i{}_j$ are determined by orthonormality conditions,

$$
\begin{aligned}
\hat{\boldsymbol{q}}_i \cdot \hat{\boldsymbol{q}}_j &:= \delta_{ij} = \sum_{k,l} M_i{}^k \, M_j{}^l \, g_{kl}, \\
\hat{\boldsymbol{q}}^i \cdot \hat{\boldsymbol{q}}^j &:= \delta^{ij} = \sum_{k,l} N^i{}_k \, N^j{}_l \, g^{kl}.
\end{aligned}
\tag{87}
$$

Where the g_{kl} and g^{kl} are given by Equations (80) and (81). Furthermore, orthogonality between the orthonormal basis and dual $\hat{\boldsymbol{q}}_i \cdot \hat{\boldsymbol{q}}^j = \delta_i{}^j$, implies the transformation matrix $\mathbf{N} = \mathbf{M}^{-1}$.

We remark, by Equations (84) and (85), the basis vectors $\boldsymbol{q}_i$ and dual basis vectors $\boldsymbol{q}^i$ are strictly proportional when the metric is diagonal, $\boldsymbol{q}^i = g^{ii} \, \boldsymbol{q}_i$ and $\boldsymbol{q}_i = g_{ii} \, \boldsymbol{q}^i$. In particular, the basis and dual basis vectors are identified, $\hat{\boldsymbol{q}}^i = \hat{\boldsymbol{q}}_i$, for *every orthonormal basis set*; specifically, the Cartesian basis $\boldsymbol{e}^i = \boldsymbol{e}_i$.

B.1.4. The Covariant Differential Operator ∇

The covariant differential ∇ is a differential operator that satisfies the standard axioms (see e.g., Kobayashi & Nomizu, 1963, p. 123-124). In curvilinear coordinates, ∇ is represented with respect to the dual basis $\boldsymbol{q}^i$ via its action on smooth functions of position q^i.

Let $f : \mathbb{R}^3 \rightarrow \mathbb{R}$ be a differentiable scalar function, then the covariant differential of f is

$$\nabla f \ = \ \sum_j \ (\ \nabla_j \ f \ ) \, \boldsymbol{q}^j = \sum_j \ \frac{\partial f}{\partial q^j} \ \boldsymbol{q}^j \tag{88}$$

(see e.g., Kobayashi & Nomizu, 1963, p. 143); in Cartesian coordinates, x^i, the basis and dual are identified, $\boldsymbol{e}^i = \boldsymbol{e}_i$, and Equation (88) reduces to the standard gradient. Furthermore, the standard differential is given by,

$$\mathrm{d}f \ = \ \mathrm{d}\boldsymbol{s} \cdot \nabla f = \sum_{i,j} \ \mathrm{d}q^i \ \frac{\partial f}{\partial q^j} \ (\ \boldsymbol{q}_i \cdot \boldsymbol{q}^j \ ) = \sum_i \ \mathrm{d}q^i \ \frac{\partial f}{\partial q^i}, \tag{89}$$

where $\mathrm{d}\boldsymbol{s} = \sum_i \ \mathrm{d}q^i \ \boldsymbol{q}_i$, and by Equation (76), $\boldsymbol{q}^i \cdot \boldsymbol{q}_j := \delta^i{}_j$.

Since the local basis $\boldsymbol{q}_i$ are themselves smooth functions of position q^i, the action of the operator ∇ on the basis vectors is a linear operation,

$$\nabla \boldsymbol{q}_i \ = \ \sum_j (\ \nabla_j \ \boldsymbol{q}_i \ ) \, \boldsymbol{q}^j = \sum_{j,k} \ \Gamma^k{}_{ji} \ \boldsymbol{q}_k \otimes \boldsymbol{q}^j. \tag{90}$$

where the linear connection coefficients are functions of position, $\Gamma^k{}_{ji} = \Gamma^k{}_{ji} \left(q^l \right)$ (see e.g., Kobayashi & Nomizu, 1963, p. 143).

A vector field $\boldsymbol{B}$ is a linear combination of smooth component functions $B^i = B^i \left(q^j, t \right)$ with respect to the basis $\boldsymbol{q}_i$,

$$\boldsymbol{B} \ = \ \sum_i \ B^i \ \boldsymbol{q}_i. \tag{91}$$

The covariant differential $\nabla \boldsymbol{B}$ of the vector field $\boldsymbol{B}$ is, then

$$\begin{aligned}
\nabla \boldsymbol{B} \ &= \ \sum_j \ \nabla_j \left(\ \sum_i \ B^i \ \boldsymbol{q}_i \ \right) \boldsymbol{q}^j \\
&= \ \sum_{i,j} \left(\ (\ \nabla_j \ B^i \ ) \, \boldsymbol{q}_i + B^i \, (\ \nabla_j \ \boldsymbol{q}_i \ ) \ \right) \boldsymbol{q}^j \\
&= \ \sum_{i,j} \left(\ \frac{\partial B^i}{\partial q^j} \ \boldsymbol{q}_i + B^i \left(\ \sum_k \ \Gamma^k{}_{ji} \ \boldsymbol{q}_k \ \right) \ \right) \boldsymbol{q}^j \\
&= \ \sum_{i,j} \ \frac{\partial B^i}{\partial q^j} \ \boldsymbol{q}_i \otimes \boldsymbol{q}^j + \sum_{i,j,k} \ \Gamma^i{}_{jk} \ B^k \ \boldsymbol{q}_i \otimes \boldsymbol{q}^j
\end{aligned}$$

$$= \sum_{i,j} \left(\frac{\partial B^i}{\partial q^j} + \sum_k \Gamma^i{}_{jk} \, B^k \right) \boldsymbol{q}_i \otimes \boldsymbol{q}^j \qquad (92)$$

Where we used Equations (88) and (90) in the second step, and relabeled dummy summation indices in the third step. Hence, the i, j-th component of the matrix representation of $\nabla \boldsymbol{B}\,(\boldsymbol{r})$ with respect to the local basis $\boldsymbol{q}_i \otimes \boldsymbol{q}^i$ is Equation (21),

$$(\, \nabla \boldsymbol{B} \,)^i{}_j \;=\; \frac{\partial B^i}{\partial q^j} + \sum_k \Gamma^i{}_{jk} \, B^k$$

(see e.g., Kobayashi & Nomizu, 1963, p. 144).

The matrix representation of the covariant differential with respect to general curvilinear bases explicitly includes terms that describe both the rate of change of the vector components, as well as the manner in which the bases vectors change from point-to-point in the system.

The determination of the linear connection coefficients Γ depends on the nature of the basis vectors. In the case of a curvilinear coordinate basis, the linear connection coefficients $\Gamma^i{}_{jk}$ may be written explicitly in terms of coordinate derivatives of the metric,

$$\Gamma^i{}_{jk} = \frac{1}{2} \sum_m g^{im} \left(\frac{\partial g_{mj}}{\partial q^k} + \frac{\partial g_{mk}}{\partial q^j} - \frac{\partial g_{jk}}{\partial q^m} \right). \qquad (93)$$

(see e.g., Kobayashi & Nomizu, 1963, p. 160).

In the case of an orthonormal basis, the linear connection coefficients $\Gamma^i{}_{jk}$ are given by,

$$\Gamma^i{}_{jk} \;=\; \frac{1}{2} \sum_m \delta^{im} \left(\, c_{kmj} + c_{jmk} - c_{mjk} \,\right). \qquad (94)$$

(see e.g., Kobayashi & Nomizu, 1963, p. 78). The c_{ijk} in Equation (93) are called *structure constants*, and are determined by the smooth component functions and derivatives of the transformation matrices in Equation (86); explicitly,

$$c_{ij}{}^k \;=\; \sum_{m,n} \left(M_i{}^m \, \frac{\partial M_j{}^n}{\partial q^m} \, (M^{-1})_n{}^k - M_j{}^n \, \frac{\partial M_i{}^m}{\partial q^n} \, (M^{-1})_m{}^k \right). \qquad (95)$$

Since, in general, the components and their derivatives of the transformation matrices are functions of position, so also are the structure constants functions of position, $c_{ij}{}^k = c_{ij}{}^k \left(q^l \right)$.

Finally, in the case of the *Cartesian basis*, the basis and dual basis are independent of position, and hence the linear connection coefficients are all trivial, $\Gamma = 0$. Therefore, for vectors with components constructed with respect to a Cartesian basis, the covariant differential reduces to the standard partial derivatives with respect to the Cartesian coordinates, see e.g., Equation (15).

B.2. Spherical-Polar Coordinate Basis

The position of each point $p \in M$ is written in terms of the spherical-polar curvilinear coordinate functions,

$$\boldsymbol{r}(p) = \{ r(p), \theta(p), \phi(p) \} \tag{96}$$

with $r \in [\, 0, \infty\,)$, $\theta \in [\, 0, \pi\,]$, and $\phi \in [\, 0, 2\pi\,)$. The Cartesian-spherical-polar coordinate transformation functions are

$$\begin{aligned}
x &= r\,\sin\theta\,\cos\phi, \\
y &= r\,\sin\theta\,\sin\phi, \\
z &= r\,\cos\theta.
\end{aligned} \tag{97}$$

The position vector is written,

$$\begin{aligned}
\boldsymbol{r} &= x\,\hat{\boldsymbol{e}}_x + y\,\hat{\boldsymbol{e}}_y + z\,\hat{\boldsymbol{e}}_z \\
&= (\,r\,\sin\theta\,\cos\phi\,)\,\hat{\boldsymbol{e}}_x + (\,r\,\sin\theta\,\sin\phi\,)\,\hat{\boldsymbol{e}}_y + (\,r\,\cos\theta\,)\,\hat{\boldsymbol{e}}_z.
\end{aligned} \tag{98}$$

Hence, using the definition of the coordinate basis vectors (72), the spherical-polar coordinate basis vectors are written in components with respect to the standard Cartesian basis,

$$\begin{aligned}
\boldsymbol{e}_r &= \sin\theta\,\cos\phi\,\hat{\boldsymbol{e}}_x + \sin\theta\,\sin\phi\,\hat{\boldsymbol{e}}_y + \cos\theta\,\hat{\boldsymbol{e}}_z, \\
\boldsymbol{e}_\theta &= r\,\cos\theta\,\cos\phi\,\hat{\boldsymbol{e}}_x + r\,\cos\theta\,\sin\phi\,\hat{\boldsymbol{e}}_y - r\,\sin\theta\,\hat{\boldsymbol{e}}_z, \\
\boldsymbol{e}_\phi &= -r\,\sin\theta\,\sin\phi\,\hat{\boldsymbol{e}}_x + r\,\sin\theta\,\cos\phi\,\hat{\boldsymbol{e}}_y.
\end{aligned} \tag{99}$$

Using Equation (80) and the fact that the Cartesian basis are orthonormal, the metric components are immediately identified,

$$\boldsymbol{e}_r \cdot \boldsymbol{e}_r = g_{rr} = 1, \quad \boldsymbol{e}_\theta \cdot \boldsymbol{e}_\theta = g_{\theta\theta} = r^2, \quad \boldsymbol{e}_\phi \cdot \boldsymbol{e}_\phi = g_{\phi\phi} = r^2 \sin^2\theta. \tag{100}$$

All other scalar products are zero. Hence, the spherical-polar coordinate basis vectors $\{\,\boldsymbol{e}_r, \boldsymbol{e}_\theta, \boldsymbol{e}_\phi\,\}$ are orthogonal, but not orthonormal. Furthermore, the inverse metric components follow immediately,

$$g^{rr} = 1, \quad g^{\theta\theta} = \frac{1}{r^2}, \quad g^{\phi\phi} = \frac{1}{r^2 \sin^2\theta}. \tag{101}$$

We construct the dual basis using Equation (85) with the inverse metric components (101),

$$\boldsymbol{e}^r = \boldsymbol{e}_r, \quad \boldsymbol{e}^\theta = \frac{\boldsymbol{e}_\theta}{r^2}, \quad \boldsymbol{e}^\phi = \frac{\boldsymbol{e}_\phi}{r^2 \sin^2\theta}. \tag{102}$$

Since the metric and inverse components are not orthonormal, the linear connection coefficients are determined by Equation (93). The only non-trivial metric component derivatives are

$$\frac{\partial g_{\theta\theta}}{\partial r} = 2r, \quad \frac{\partial g_{\phi\phi}}{\partial r} = 2r \sin^2\theta, \quad \frac{\partial g_{\phi\phi}}{\partial \theta} = 2r^2 \sin\theta\cos\theta. \tag{103}$$

Hence, the non-zero linear connection components are

$$\Gamma^r{}_{\theta\theta} = -r, \qquad \Gamma^r{}_{\phi\phi} = -r\sin^2\theta,$$

$$\Gamma^\theta{}_{r\theta} = \Gamma^\theta{}_{\theta r} = \frac{1}{r}, \qquad \Gamma^\theta{}_{\phi\phi} = -\sin\theta\cos\theta,$$

$$\Gamma^\phi{}_{r\phi} = \Gamma^\phi{}_{\phi r} = \frac{1}{r}, \qquad \Gamma^\phi{}_{\theta\phi} = \Gamma^\phi{}_{\phi\theta} = \cot\theta. \tag{104}$$

Thus, with respect to the spherical-polar curvilinear basis the vector field is

$$\boldsymbol{B} = B^r\,(r,\theta,\phi)\,\boldsymbol{e}_r + B^\theta\,(r,\theta,\phi)\,\boldsymbol{e}_\theta + B^\phi\,(r,\theta,\phi)\,\boldsymbol{e}_\phi, \tag{105}$$

and the matrix representation of the covariant differential $\nabla\boldsymbol{B}$, Equation (21), is

$$(\,\nabla\boldsymbol{B}\,)^i{}_j \;=\; \begin{pmatrix} \dfrac{\partial B^r}{\partial r} & \dfrac{\partial B^r}{\partial\theta} - r\,B^\theta & \dfrac{\partial B^r}{\partial\phi} - r\sin^2\theta\,B^\phi \\[3ex] \dfrac{\partial B^\theta}{\partial r} & \dfrac{\partial B^\theta}{\partial\theta} + \dfrac{B^r}{r} & \dfrac{\partial B^\theta}{\partial\phi} - \sin\theta\cos\theta\,B^\phi \\[3ex] \dfrac{\partial B^\phi}{\partial r} + \dfrac{B^\phi}{r} & \dfrac{\partial B^\phi}{\partial\theta} + \cot\theta\,B^\phi & \dfrac{\partial B^\phi}{\partial\phi} + \dfrac{B^r}{r} + \cot\theta\,B^\theta \end{pmatrix}. \tag{106}$$

B.3. Spherical-Polar Orthonormal Basis

The position of each point $p \in M$ is written in terms of the spherical-polar coordinate functions, Equation (96),

$$\boldsymbol{r}\,(p) \;=\; \{\,r\,(p)\,,\theta\,(p)\,,\phi\,(p)\,\}$$

with $r \in [\,0,\infty\,)$, $\theta \in [\,0,\pi\,]$, and $\phi \in [\,0,2\pi\,)$.

By Equations (86), the spherical-polar coordinate basis, Equation (99), respectively dual basis, Equation (102), may be orthonormalized using the transformation matrices $\mathbf{M}$ and $\mathbf{N}$,

$$\mathbf{M} = \begin{pmatrix} 1 & 0 & 0 \\ 0 & \dfrac{1}{r} & 0 \\ 0 & 0 & \dfrac{1}{r\sin\theta} \end{pmatrix}, \;\; \text{resp.}\;\; \mathbf{N} = \mathbf{M}^{-1} = \begin{pmatrix} 1 & 0 & 0 \\ 0 & r & 0 \\ 0 & 0 & r\sin\theta \end{pmatrix}. \tag{107}$$

The spherical-polar orthogonal basis, respectively dual basis, are defined by linear combinations of the spherical-polar curvilinear basis,

$$\hat{\boldsymbol{e}}_r = \boldsymbol{e}_r, \quad \hat{\boldsymbol{e}}_\theta = \frac{1}{r}\,\boldsymbol{e}_\theta, \quad \hat{\boldsymbol{e}}_\phi = \frac{1}{r\sin\theta}\,\boldsymbol{e}_\phi, \tag{108}$$

respectively dual basis,

$$\hat{\boldsymbol{e}}^r = \boldsymbol{e}^r, \quad \hat{\boldsymbol{e}}^\theta = r\,\boldsymbol{e}^\theta, \quad \hat{\boldsymbol{e}}^\phi = r\sin\theta\,\boldsymbol{e}^\phi. \tag{109}$$

The transformation matrices, Equation (107), were constructed specifically so that with respect to the basis (108) and dual basis (109), the metric and inverse components are, respectively, $g_{ij} = \delta_{ij}$ and $g^{ij} = \delta^{ij}$. Hence, the linear connection coefficients are determined by Equation (94). In this case, the non-zero structure constants determined by Equation (95) are

$$c_{r\theta\theta} = -c_{\theta r\theta} = c_{r\phi\phi} = -c_{\phi r\phi} = -\frac{1}{r}, \quad c_{\theta\phi\phi} = -c_{\phi\theta\phi} = -\frac{\cot\theta}{r}. \tag{110}$$

Hence, the non-zero linear connection components are

$$\Gamma^{\theta}{}_{r\theta} = \Gamma^{\phi}{}_{r\phi} = -\Gamma^{r}{}_{\theta\theta} = -\Gamma^{r}{}_{\phi\phi} = \frac{1}{r},$$

$$\Gamma^{\phi}{}_{\theta\phi} = -\Gamma^{\theta}{}_{\phi\phi} = \frac{\cot\theta}{r}. \tag{111}$$

Thus, with respect to the spherical-polar orthonormal basis the vector field is

$$\boldsymbol{B} = B^{r}(r,\theta,\phi)\,\hat{\boldsymbol{e}}_{r} + B^{\theta}(r,\theta,\phi)\,\hat{\boldsymbol{e}}_{\theta} + B^{\phi}(r,\theta,\phi)\,\hat{\boldsymbol{e}}_{\phi} \tag{112}$$

and the matrix representation of the covariant differential $\nabla\boldsymbol{B}$, Equation (21), is

$$(\nabla\boldsymbol{B})^{i}{}_{j} = \begin{pmatrix} \dfrac{\partial B^{r}}{\partial r} & \dfrac{1}{r}\dfrac{\partial B^{r}}{\partial\theta} - \dfrac{B^{\theta}}{r} & \dfrac{1}{r\sin\theta}\dfrac{\partial B^{r}}{\partial\phi} - \dfrac{B^{\phi}}{r} \\[2ex] \dfrac{\partial B^{\theta}}{\partial r} & \dfrac{1}{r}\dfrac{\partial B^{\theta}}{\partial\theta} + \dfrac{B^{r}}{r} & \dfrac{1}{r\sin\theta}\dfrac{\partial B^{\theta}}{\partial\phi} - \dfrac{\cot\theta\, B^{\phi}}{r} \\[2ex] \dfrac{\partial B^{\phi}}{\partial r} & \dfrac{1}{r}\dfrac{\partial B^{\phi}}{\partial\theta} & \dfrac{1}{r\sin\theta}\dfrac{\partial B^{\phi}}{\partial\phi} + \dfrac{B^{r}}{r} + \dfrac{\cot\theta\, B^{\theta}}{r} \end{pmatrix}. \tag{113}$$

C. On the Determinant of the Matrix Representation of a Smooth, Non-Singular, Linear Map F

In this appendix, we prove Equations (30) and (33) involving the determinant of a square matrix. In particular, given a linear map $\mathbf{F}$, in Appendix C.1 we show the determinant of the matrix representation of $\mathbf{F}$ in an arbitrary proper orthonormal basis is given by the ratio of (signed) differential volume elements in bases related by the action of the transformation $\mathbf{F}$. In Appendix C.2, assuming well-posed ordinary differential equations describing the evolution of the matrix representation of a linear map $\mathbf{F}$, we calculate the rate of change of the determinant with respect to the evolution parameter. Furthermore, this treatment is independent of basis used to construct the matrix representation of $\mathbf{F}$.

Since we are dealing with the 3×3 matrix representation of a linear map $\mathbf{F}$, throughout this Appendix we make use of the permutation group S_3 applied to the components of the matrix. The permutation group S_3 contains $3! = 6$

elements, $S_3 = \{ \sigma_1, \ldots, \sigma_6 \}$; written in a tabular format, we show the action of each element $\sigma_i \in S_3$ as a column vector

$$
\begin{array}{c|c|c|c|c|c|c}
S_3 & \sigma_1 & \sigma_2 & \sigma_3 & \sigma_4 & \sigma_5 & \sigma_6 \\
\hline
\sigma_i\,(1) & 1 \to 1 & 1 \to 2 & 1 \to 1 & 1 \to 3 & 1 \to 2 & 1 \to 3 \\
\sigma_i\,(2) & 2 \to 2 & 2 \to 1 & 2 \to 3 & 2 \to 2 & 2 \to 3 & 2 \to 1 \\
\sigma_i\,(3) & 3 \to 3 & 3 \to 3 & 3 \to 2 & 3 \to 1 & 3 \to 1 & 3 \to 2
\end{array}
\tag{114}
$$

Each $\sigma_i \in S_3$ may be considered as a function that transposes the labels $(1, 2, 3)$. Consider, for example, σ_2 denoted by the second column: $\sigma_2\,(1) = 2$, $\sigma_2\,(2) = 1$, and $\sigma_2\,(3) = 3$. That is, σ_2 exchanges indices 1 and 2.

The determinant of any 3×3 matrix may be written in terms of the S_3 permutation group[5],

$$
\det \mathbf{F} \;=\; \sum_{\sigma_i \in S_3} \mathrm{sign}\,(\sigma_i) \prod_{j=1}^{3} F_{j\sigma_i(j)},
\tag{115}
$$

where $\mathrm{sign} : S_3 \to \{\pm 1\}$ is the function $\mathrm{sign}\,(\sigma_i) = (-1)^n$ such that n is the number of transpositions between adjacent labels needed to return from σ_i to $\sigma_1 = (1, 2, 3)$; for example, $\mathrm{sign}\,(\sigma_2) = (-1)^1 = -1$ since $\sigma_2 = (2, 1, 3)$ requires one transposition between labels 2 and 1 to match $\sigma_1 = (1, 2, 3)$. Explicitly, given the labels defined by (114),

$$
\begin{aligned}
\mathrm{sign}\,(\sigma_1) = \mathrm{sign}\,(\sigma_5) = \mathrm{sign}\,(\sigma_6) \;&=\; +1, \\
\mathrm{sign}\,(\sigma_2) = \mathrm{sign}\,(\sigma_3) = \mathrm{sign}\,(\sigma_4) \;&=\; -1.
\end{aligned}
\tag{116}
$$

We note, Equation (115) is independent of the basis in which the matrix $\mathbf{F}$ is represented. Furthermore, the index position in which the pair $(\, j, \sigma_i\,(j)\,)$ appears is irrelevant.

C.1. Calculating the Determinant of a Non-Singular, 3×3 Matrix F Via Identity (30) for Arbitrary Proper Orthonormal Bases.

Let (M, h^i) with $M \subseteq \mathbb{R}^3$ be a coordinate chart, such that with respect to a proper orthonormal basis $\boldsymbol{h}_i$, the coordinate differential basis vectors are $\mathrm{d}\boldsymbol{h}^i = \mathrm{d}h^i\,\boldsymbol{h}_i$. Since the basis $\boldsymbol{h}_i$ is proper, then $\boldsymbol{h}_3 \cdot (\,\boldsymbol{h}_1 \times \boldsymbol{h}_2\,) = 1$. Written in this basis, the signed differential volume element is

$$
\begin{aligned}
\mathrm{d}\Omega\,(\boldsymbol{h}_i) \;&=\; \mathrm{d}\boldsymbol{h}^3 \cdot (\,\mathrm{d}\boldsymbol{h}^1 \times \mathrm{d}\boldsymbol{h}^2\,) \\
&=\; (\,\mathrm{d}h^3\,\boldsymbol{h}_3\,) \cdot (\,(\,\mathrm{d}h^1\,\boldsymbol{h}_1\,) \times (\,\mathrm{d}h^2\,\boldsymbol{h}_2\,)\,) \\
&=\; \boldsymbol{h}_3 \cdot (\,\boldsymbol{h}_1 \times \boldsymbol{h}_2\,)\;\mathrm{d}h^1\,\mathrm{d}h^2\,\mathrm{d}h^3 \\
&=\; \mathrm{d}h^1\,\mathrm{d}h^2\,\mathrm{d}h^3.
\end{aligned}
\tag{117}
$$

---

[5]More generally, the determinant of any $n \times n$ matrix may be similarly written in terms of the S_n permutation group.

Suppose the linear map $\mathbf{F}$ may be represented as a non-singular, 3×3 matrix with respect to this general proper orthonormal basis $\boldsymbol{h}_i$ and dual basis $\boldsymbol{h}^i$ (see Appendix B.1),

$$\mathbf{F} = \sum_{i,j} F^i{}_j \ \boldsymbol{h}_i \otimes \boldsymbol{h}^j. \tag{118}$$

Since $\mathbf{F}$ is non-singular, its action is completely described by the transformation of the basis vectors. The propagated coordinate differentials follow immediately,

$$\mathrm{d}\boldsymbol{v}^i \ = \ \mathbf{F} \cdot \mathrm{d}\boldsymbol{h}^i = \sum_j F^j{}_i \ \mathrm{d}h^i \ \boldsymbol{h}_j. \tag{119}$$

We note, in general, for $\det \mathbf{F} > 0$, the propagated basis $\boldsymbol{v}_i$ is not orthonormal, though the orientation is preserved.

The signed differential volume element with respect to the $\boldsymbol{v}_i$ basis is then

$$
\begin{aligned}
\mathrm{d}\Omega\left(\boldsymbol{v}_i\right) \ &= \ \mathrm{d}\boldsymbol{v}^3 \cdot \left(\ \mathrm{d}\boldsymbol{v}^1 \times \mathrm{d}\boldsymbol{v}^2\ \right) \\
&= \left(\sum_k F^k{}_3 \ \mathrm{d}h^3 \ \boldsymbol{h}_k \right) \cdot \left(\left(\sum_i F^i{}_1 \ \mathrm{d}h^1 \ \boldsymbol{h}_i \right) \times \left(\sum_j F^j{}_2 \ \mathrm{d}h^2 \ \boldsymbol{h}_j \right) \right) \\
&= \sum_{i,j,k} F^i{}_1 \ F^j{}_2 \ F^k{}_3 \ \boldsymbol{h}_k \cdot \left(\ \boldsymbol{h}_i \times \boldsymbol{h}_j\ \right) \ \mathrm{d}h^1 \ \mathrm{d}h^2 \ \mathrm{d}h^3 \\
&= \sum_{i,j,k} F^i{}_1 \ F^j{}_2 \ F^k{}_3 \ \boldsymbol{h}_k \cdot \left(\ \boldsymbol{h}_i \times \boldsymbol{h}_j\ \right) \ \mathrm{d}\Omega\left(\boldsymbol{h}_i\right),
\end{aligned}
\tag{120}
$$

where we used Equations (117) and (119).

Since the basis $\boldsymbol{h}_i$ is proper orthonormal, the triple vector product $\boldsymbol{h}_k \cdot \left(\ \boldsymbol{h}_i \times \boldsymbol{h}_j\ \right)$ reduces the number of terms in the i, j, k summation expansion to 6; namely, only those involving the permutations of $(i, j, k) = (1, 2, 3)$ with $i \neq j \neq k$. Hence, we renumerate the reduced i, j, k summation according to elements of the S_3 permutation group, Equation (114), (see e.g., Kobayashi & Nomizu, 1963, p. 283),

$$
\begin{aligned}
\mathrm{d}\Omega\left(\boldsymbol{v}_i\right) \ &= \ \sum_{\sigma_i \in S_3} F^{\sigma_i(1)}{}_1 \ F^{\sigma_i(2)}{}_2 \ F^{\sigma_i(3)}{}_3 \ \boldsymbol{h}_{\sigma_i(3)} \cdot \left(\ \boldsymbol{h}_{\sigma_i(1)} \times \boldsymbol{h}_{\sigma_i(2)}\ \right) \ \mathrm{d}\Omega\left(\boldsymbol{h}_i\right) \\
&= \ \sum_{\sigma_i \in S_3} F^{\sigma_i(1)}{}_1 \ F^{\sigma_i(2)}{}_2 \ F^{\sigma_i(3)}{}_3 \left(\ \mathrm{sign}\left(\sigma_i\right) \ \boldsymbol{h}_3 \cdot \left(\ \boldsymbol{h}_1 \times \boldsymbol{h}_2\ \right)\ \right) \ \mathrm{d}\Omega\left(\boldsymbol{h}_i\right) \\
&= \left(\sum_{\sigma_i \in S_3} \mathrm{sign}\left(\sigma_i\right) \ F^{\sigma_i(1)}{}_1 \ F^{\sigma_i(2)}{}_2 \ F^{\sigma_i(3)}{}_3 \right) \ \mathrm{d}\Omega\left(\boldsymbol{h}_i\right) \\
&= \left(\sum_{\sigma_i \in S_3} \mathrm{sign}\left(\sigma_i\right) \prod_j F^{\sigma_i(j)}{}_j \right) \ \mathrm{d}\Omega\left(\boldsymbol{h}_i\right) \\
&= \ \det \mathbf{F} \ \mathrm{d}\Omega\left(\boldsymbol{h}_i\right).
\end{aligned}
\tag{121}
$$

Example: Consider the Cartesian basis $\{\, \boldsymbol{e}_x, \boldsymbol{e}_y, \boldsymbol{e}_z \,\}$ with $\boldsymbol{e}_z \cdot (\, \boldsymbol{e}_x \times \boldsymbol{e}_y \,) = 1$. The differential basis vectors are $\mathrm{d}\boldsymbol{x}^i = \mathrm{d}x^i\, \boldsymbol{e}_i$. Hence, the initial differential volume element, (26), is given by

$$
\begin{aligned}
\mathrm{d}\Omega_0 &= (\, \mathrm{d}z\, \boldsymbol{e}_z \,) \cdot (\, (\, \mathrm{d}x\, \boldsymbol{e}_x \,) \times (\, \mathrm{d}y\, \boldsymbol{e}_y \,) \,) \\
&= \boldsymbol{e}_z \cdot (\, \boldsymbol{e}_x \times \boldsymbol{e}_y \,)\ \mathrm{d}x\, \mathrm{d}y\, \mathrm{d}z \\
&= \mathrm{d}x\, \mathrm{d}y\, \mathrm{d}z.
\end{aligned}
\tag{122}
$$

Furthermore, the differential volume element, (29), propagated along the congruence by the 3×3 matrix $\mathbf{F}$ is,

$$
\begin{aligned}
\mathrm{d}\Omega_\lambda &= (\, \mathbf{F} \cdot \mathrm{d}\boldsymbol{z} \,) \cdot (\, (\, \mathbf{F} \cdot \mathrm{d}\boldsymbol{x} \,) \times (\, \mathbf{F} \cdot \mathrm{d}\boldsymbol{y} \,) \,) \\
&= (\, \mathrm{d}z\, \mathbf{F} \cdot \boldsymbol{e}_z \,) \cdot (\, (\, \mathrm{d}x\, \mathbf{F} \cdot \boldsymbol{e}_x \,) \times (\, \mathrm{d}y\, \mathbf{F} \cdot \boldsymbol{e}_y \,) \,) \\
&= (\, \mathbf{F} \cdot \boldsymbol{e}_z \,) \cdot (\, (\, \mathbf{F} \cdot \boldsymbol{e}_x \,) \times (\, \mathbf{F} \cdot \boldsymbol{e}_y \,) \,)\ \mathrm{d}x\, \mathrm{d}y\, \mathrm{d}z \\
&= (\, \mathbf{F} \cdot \boldsymbol{e}_z \,) \cdot (\, (\, \mathbf{F} \cdot \boldsymbol{e}_x \,) \times (\, \mathbf{F} \cdot \boldsymbol{e}_y \,) \,)\ \mathrm{d}\Omega_0.
\end{aligned}
\tag{123}
$$

The general 3×3 matrix components of $\mathbf{F}$ with respect to the (Cartesian) basis $\boldsymbol{e}_i \otimes \boldsymbol{e}^j$ are,

$$
F^i{}_j = \begin{pmatrix}
F^x{}_x & F^x{}_y & F^x{}_z \\
F^y{}_x & F^y{}_y & F^y{}_z \\
F^z{}_x & F^z{}_y & F^z{}_z
\end{pmatrix}.
\tag{124}
$$

The action of the 3×3 matrix $\mathbf{F}$ on the basis vectors is,

$$
\mathbf{F} \cdot \boldsymbol{e}_i = F^x{}_i\, \boldsymbol{e}_x + F^y{}_i\, \boldsymbol{e}_y + F^z{}_i\, \boldsymbol{e}_z.
\tag{125}
$$

Then,

$$
\begin{aligned}
(\, \mathbf{F} \cdot \boldsymbol{e}_x \,) \times (\, \mathbf{F} \cdot \boldsymbol{e}_y \,) &= (\, F^y{}_x\, F^z{}_y - F^z{}_x\, F^y{}_y \,)\, \boldsymbol{e}_x \\
&\quad + (\, F^z{}_x\, F^x{}_y - F^x{}_x\, F^z{}_y \,)\, \boldsymbol{e}_y \\
&\quad + (\, F^x{}_x\, F^y{}_y - F^y{}_x\, F^x{}_y \,)\, \boldsymbol{e}_z.
\end{aligned}
\tag{126}
$$

Hence, the triple vector product of the orthonormal Cartesian basis $\boldsymbol{e}_i$ under the action of the linear map $\mathbf{F}$ is the determinant of the 3×3 matrix of $\mathbf{F}$ with the usual meaning,

$$
\begin{aligned}
(\, \mathbf{F} \cdot \boldsymbol{e}_z \,) \cdot (\, (\, \mathbf{F} \cdot \boldsymbol{e}_x \,) \times (\, \mathbf{F} \cdot \boldsymbol{e}_y \,) \,) &= F^x{}_z\, (\, F^y{}_x\, F^z{}_y - F^z{}_x\, F^y{}_y \,) \\
&\quad + F^y{}_z\, (\, F^z{}_x\, F^x{}_y - F^x{}_x\, F^z{}_y \,) \\
&\quad + F^z{}_z\, (\, F^x{}_x\, F^y{}_y - F^y{}_x\, F^x{}_y \,) \\
&= \det \mathbf{F}.
\end{aligned}
\tag{127}
$$

Finally, combining Equations (123) and (127), we recover Equation (30).

C.2. Differentiation of the Determinant of a Smooth, Non-Singular, Linear Map $\mathbf{F}(\lambda)$

In this Appendix we demonstrate Equation (33) for the determinant of a square (3×3) matrix-valued function of a single real parameter, $\mathbf{F}(\lambda)$.

Let $\mathbf{F}, \mathbf{M} : \mathbb{R} \to \mathbb{R}^{3 \times 3}$ be smooth, non-singular, linear, 3×3 matrix-valued functions of λ; that is, the components $F_{ij}(\lambda)$ and $M_{ij}(\lambda)$ with respect to any basis representation are at least C^1-functions. Furthermore, assume $\mathbf{F}(\lambda)$ and $\mathbf{M}(\lambda)$ satisfy the linear matrix ordinary differential equations for all $\lambda \in \mathbb{R}$; in components with respect to any basis

$$\frac{\partial F_{ij}(\lambda)}{\partial \lambda} = \sum_k M_{ik}(\lambda) \ F_{kj}(\lambda), \tag{128}$$

$$F_{ij}(0) = (F_0)_{ij}. \tag{129}$$

Equations (128) and (129) are a generalization of Equations (16) and (17). In particular, $M_{ij}(\lambda) = (\left.\nabla \boldsymbol{B}\right|_{\boldsymbol{r}})^i{}_j$ with $\boldsymbol{r} = \boldsymbol{r}(\lambda, \boldsymbol{r}_0)$, and initial condition $(F_0)_{ij} = \delta^i{}_j$. However, the following results are general, independent of the specifics of the basis representation and physical vector fields.

Hence, writing $\det \mathbf{F}$ with Equation (115), and differentiating with respect to the λ-parameter,

$$
\begin{aligned}
\frac{\partial \det \mathbf{F}}{\partial \lambda} &= \frac{\partial}{\partial \lambda} \left(\sum_{\sigma_i \in S_3} \text{sign}(\sigma_i) \prod_j F_{j\sigma_i(j)} \right) \\
&= \sum_{\sigma_i \in S_3} \text{sign}(\sigma_i) \frac{\partial}{\partial \lambda} \left(F_{1\sigma_i(1)} \ F_{2\sigma_i(2)} \ F_{3\sigma_i(3)} \right) \\
&= \sum_{\sigma_i \in S_3} \text{sign}(\sigma_i) \left(\frac{\partial F_{1\sigma_i(1)}}{\partial \lambda} \ F_{2\sigma_i(2)} \ F_{3\sigma_i(3)} \right) \\
&+ \sum_{\sigma_i \in S_3} \text{sign}(\sigma_i) \left(F_{1\sigma_i(1)} \ \frac{\partial F_{2\sigma_i(2)}}{\partial \lambda} \ F_{3\sigma_i(3)} \right) \\
&+ \sum_{\sigma_i \in S_3} \text{sign}(\sigma_i) \left(F_{1\sigma_i(1)} \ F_{2\sigma_i(2)} \ \frac{\partial F_{3\sigma_i(3)}}{\partial \lambda} \right).
\end{aligned}
$$

Using Equation (128),

$$
\begin{aligned}
\frac{\partial \det \mathbf{F}}{\partial \lambda} &= \sum_{\sigma_i \in S_3} \text{sign}(\sigma_i) \left(\sum_k M_{1k} \ F_{k\sigma_i(1)} \right) F_{2\sigma_i(2)} \ F_{3\sigma_i(3)} \\
&+ \sum_{\sigma_i \in S_3} \text{sign}(\sigma_i) \ F_{1\sigma_i(1)} \left(\sum_k M_{2k} \ F_{k\sigma_i(2)} \right) F_{3\sigma_i(3)} \\
&+ \sum_{\sigma_i \in S_3} \text{sign}(\sigma_i) \ F_{1\sigma_i(1)} \ F_{2\sigma_i(2)} \left(\sum_k M_{3k} \ F_{k\sigma_i(3)} \right). \tag{130}
\end{aligned}
$$

All terms in Equation (130) which are *not* of the form $F_{1\sigma_i(1)}\ F_{2\sigma_i(2)}\ F_{3\sigma_i(3)}$ cancel as follows. Consider the coefficient of each M_{ak} component. We may write Equation (130) as

$$\frac{\partial \det \mathbf{F}}{\partial \lambda} \ = \ \sum_{a,k} C_{ak}\ M_{ak}, \tag{131}$$

where the coefficients C_{ak} are defined,

$$C_{1k} := \sum_{\sigma_i \in S_3} \text{sign}\,(\sigma_i)\, F_{k\sigma_i(1)}\ F_{2\sigma_i(2)}\ F_{3\sigma_i(3)},$$

$$C_{2k} := \sum_{\sigma_i \in S_3} \text{sign}\,(\sigma_i)\, F_{1\sigma_i(1)}\ F_{k\sigma_i(2)}\ F_{3\sigma_i(3)},$$

$$C_{3k} := \sum_{\sigma_i \in S_3} \text{sign}\,(\sigma_i)\, F_{1\sigma_i(1)}\ F_{2\sigma_i(2)}\ F_{k\sigma_i(3)}, \tag{132}$$

Each coefficient, Equation (132), is constructed by combinations of the group elements along with their respective sign functions. Then by a judicious regrouping of the summation terms, $C_{ak} = 0$ for $a \neq k$.

For example, consider the coefficient C_{1k} with $k = 2$. Upon expanding the summation, we may regroup the terms by paring the same value of $\sigma_i(3)$ in Table (114), which defines the ensemble $A_3 = \{(\sigma_1, \sigma_2), (\sigma_6, \sigma_3), (\sigma_5, \sigma_4)\}$. Then the coefficient C_{12} can be rewritten as,

$$C_{12} := \sum_{\sigma_i \in S_3} \text{sign}\,(\sigma_i)\, F_{2\sigma_i(1)}\ F_{2\sigma_i(2)}\ F_{3\sigma_i(3)}$$

$$= \sum_{(\sigma_i, \sigma_j) \in A_3} \big(F_{2\sigma_i(1)}\ F_{2\sigma_i(2)} - F_{2\sigma_j(1)}\ F_{2\sigma_j(2)} \big)\, F_{3\sigma_i(3)}. \tag{133}$$

Where the $F_{3\sigma_i(3)}$ term may be factored for each pair, since $\sigma_i(3) = \sigma_j(3)$ for all $i, j = 1, 2, 3$. Furthermore, each pair $(\sigma_i, \sigma_j) \in A_3$ satisfies $\sigma_i(1) = \sigma_j(2)$ and $\sigma_i(2) = \sigma_j(1)$ (see Table (114)). Then the terms in parenthesis vanish for each pair $(\sigma_i, \sigma_j) \in A_3$ and $C_{12} = 0$.

Similarly, for $k = 3$, we have $A_2 = \{(\sigma_1, \sigma_4), (\sigma_6, \sigma_2), (\sigma_5, \sigma_3)\}$ with $\sigma_i(2) = \sigma_j(2)$ for each pair, and

$$C_{13} = \sum_{(\sigma_i, \sigma_j) \in A_2} \big(F_{3\sigma_i(1)}\ F_{3\sigma_i(3)} - F_{3\sigma_j(1)}\ F_{3\sigma_j(3)} \big)\, F_{2\sigma_i(2)}$$

$$= 0. \tag{134}$$

The same arguments extend to all C_{ak} for all $a \neq k$, so that only terms C_{ak} for $a = k$ with $F_{1\sigma_i(1)}\ F_{2\sigma_i(2)}\ F_{3\sigma_i(3)}$ have non-vanishing contributions. Hence,

$$\frac{\partial \det \mathbf{F}}{\partial \lambda} \ = \ \sum_{\sigma_i \in S_3} \text{sign}\,(\sigma_i)\, (\ M_{11} + M_{22} + M_{33}\ )\, F_{1\sigma_i(1)}\ F_{2\sigma_i(2)}\ F_{3\sigma_i(3)}$$

$$= (M_{11} + M_{22} + M_{33}) \left(\sum_{\sigma_i \in S_3} \text{sign}(\sigma_i) \, F_{1\sigma_i(1)} \, F_{2\sigma_i(2)} \, F_{3\sigma_i(3)} \right)$$

$$= (\text{Tr } \mathbf{M}) \left(\sum_{\sigma_i \in S_3} \text{sign}(\sigma_i) \prod_j F_{j\sigma_i(j)} \right)$$

$$= \text{Tr } \mathbf{M} \det \mathbf{F}. \tag{135}$$

References

Abbo, L., Ofman, L., Antiochos, S.K., Hansteen, V.H., Harra, L., Ko, Y.-K., Lapenta, G., Li, B., Riley, P., Strachan, L., von Steiger, R., & Wang, Y.-M.: 2016, *Space Sci. Rev.*, **201**, 55.

Akhmetiev, P., & Ruzmaikin, A.: 1995, *J. Geom. and Phys.*, **15**, 95.

Antiochos, S.K.: 1987, *Astrophys. J.*, **312**, 886.

Antiochos, S.K.: 2013, *Astrophys. J.*, **772**, 1.

Antiochos, S.K., DeVore, C.R., & Klimchuck, J.A.: 1999, *Astrophys. J.*, **510**, 485.

Antiochos, S.K., Mikić, Z., Titov, V.S., Lionello, R., & Linker, J.A.: 2011, *Astrophys. J.*, **731**, 112.

Arge, C.N., & Pizzo, V.J.: 2000, *J. Geophys. Res.*, **105**, 10465.

Arnold, V. I.: 1974, Akademiya ArmSSR, Erevan, p. 229 - 256; Reprinted in Sei. Math. Sov., **5**, 4 (1986).

Arnold, V. I.: 1992, *Ordinary Differential Equations*. Springer.

Arnold, V. I., & Khesin, B. A.: 1998, *Topological Methods in Hydrodynamics*. Applied Mathematical Sciences, vol. 125, ed. Marsden, J. E., & Sirovich, L., Springer.

Aulanier, G., DeLuca, E.E., Antiochos, S.K., McMullen, R.A., & Golub, L.: 2000, *Astrophys. J.*, **540**, 1126.

Aulanier, G., Démoulin, P., & Grappin, R.: 2005, *Astron. Astrophys.*, **430**, 1067.

Aulanier, G., Pariat, E., & Démoulin, P.: 2005, *Astron. Astrophys.*, **444**, 961.

Aulanier, G., Pariat, E., Démoulin, P., & DeVore, C.R.: 2006, *Solar Phys.*, **238**, 347.

Aulanier, G., Török, T., Démoulin, P., & DeLuca, E.E.: 2010, *Astrophys. J.*, **708**, 314.

Berger, M.A.: 1984, *Geophys. Astrophys. Fluid Dyn.*, **30**, 79.

Berger, M.A.: 1991, *J. Phys. A: Math. Gen.*, **24**, 4027.

Berger, M.A.: 1994, *Space Sci. Rev.*, **68**, 3.

Berger, M.A., & Field, G.B.: 1984, *J. Fluid Mech.*, **147**, 133.

Berger, M.A., & Prior, C.: 2006, *J. Phys. A: Math. Gen.*, **39**, 8321.

Bernstein, D.S.: 2018, *Scalar, Vector, and Matrix Mathematics*. Princeton University Press, Princeton, New Jersey.

Brown, M.R., Canfield, R.C., & Pevtsov, A.A. eds.: 2013, *Magnetic Helicity in Space and Laboratory Plasmas*. Geophysical Monograph 111. American Geophysical Union. ISBN 0-87590-094-1.

Bulanov, S.V., & Sasorov, P.V.: 1978, *JETP Lett.*, **27**, 10, 554.

Bulanov, S.V., Echkina, E.Yn., Inovenkov, I.N., Pegoraro, F., & Pichushkin, V.V.: 1999, *Phys. Plasmas*, **6**, 3, 802.

Bulanov, S.V., Echkina, E.Yn., Inovenkov, I.N., & Pegoraro, F.,: 2002, *Phys. Plasmas*, **9**, 9, 3835.

Cranmer, S.R., van Ballegooijen, A.A., & Edgar, R.J.: 2007, *Astrophys. J. Sup. Ser.*, **171**, 2.

Démoulin, P., Hénoux, J.C., Priest, E.R., & Mandrini, C.H.: 1996, *Astron. Astrophys.*, **308**, 643.

Démoulin, P., Bagalá, L.G., Mandrini, C.H., Hénoux, J.C., & Rovira, M.G.: 1997, *Astron. Astrophys.*, **325**, 305.

Effenberger, F., Thust, K., Arnold, L., Grauer, R., & Dreher, J.: 2011, *Phys. Plasmas*, **18**, 032902.

Fisk, L.A., Schwadron, N.A., & Zurbuchen, T.H.: 1998, *Space Sci. Rev.*, **86**, 1/4, 51.

Fisk, L.A.: 2003, *J. Geophys. Res.*, **108**, 1157.

Halmos, P.R.: 1958, *Finite-Dimensional Vector Spaces, 2nd ed.*, Van Nostrand, Princeton NJ.

Hesse, M., & Schindler, K.: 1988, *J. Geophys. Res.*, **93**, 5559.

Hirsch, M.W., & Smale, S.: 1974, *Differential Equations, Dynamical Systems, and Linear Algebra*. Pure and Applied Mathematics, ed. Eilenberg, S., & Bass, H., Academic Press Inc., Harcourt Brace Jovanovich.

Hornig, G.: 1997, *Phys. Plasmas*, **4**, 3.

Hornig, G.: 1999, *Topological Constraints on the Relaxation of Complex Magnetic Fields*. The 9th European Meeting on Solar Physics. 12-18 September, 1999. Florence, Italy. Ed. A. Wilson. European Space Agency, ESA SP-448. ISBN: 92-9092-792-5.

Hornig, G., & Schindler, K.: 1996, *Phys. Plasmas*, **3**, 3.

Jackson, J.D.: 1999, *Classical Electrodynamics, 3rd ed.*, Ed., John Wiley & Sons, Inc.

Janvier, M.: 2017, *J. Plasma Phys.*, **83**, 535830101.

Janvier, M., Aulanier, G., Pariat, E., & Démoulin, P.: 2013, *Astron. Astrophys.*, **555**, A17.

Janvier, M., Aulanier, G., Bommier, V., Schmieder, B., Démoulin, P., & Pariat, E.: 2014, *Astrophys. J.*, **788**, 60.

Klimchuk, J.A.: 2006, *Solar Phys.*, **234**, 41.

Kobayashi, S., & Nomizu, K.: 1963, *Foundations of Differential Geometry, vol. 1*, John Wiley & Sons, Inc.

Lau, Y.T., & Finn, J.M.: 1990, *Astrophys. J.*, **350**, 672.

Longcope, D.W.: 2005, *Living Rev. Sol. Phys.*, 2: 7. https://doi.org/10.12942/lrsp-2005-7.

Longcope, D.W., & Cowley, S.C.: 1996, *Phys. Plasmas*, **3**, 2885.

Longcope, D.W., & Malanushenko, A.: 2007, *Astrophys. J.*, **674**, 1130.

Low, B.C.: 1987, *Astrophys. J.*, **323**, 358.

Low, B.C.: 1992, *Astron. Astrophys.*, **253**, 311.

Lynch, B.J., Antiochos, S.K., DeVore, C.R., Luhman, J.G., & Zurbuchen, T.H.: 2008, *Astrophys. J.*, **683**, 1192.

Lynch, B.J., & Edmondson, J.K.: 2013, *Astrophys. J.*, **764**, 87.

Lynch, B.J., Masson, S., Li, Y., DeVore, C.R., Luhmann, J.G., Antiochos, S.K., & Fisher, G. H.: 2016, *J. Geophys. Res.*, **121**, 11, 10667.

Mandrini, C.H., Démoulin, P., Rovira, M.G., de La Beaujardiere, J.-F., & Hénoux, J.C.: 1995, *Astron. Astrophys.*, **303**, 927.

Malanushenko, A., Longcope, D.W., Fan, Y., & Gibson, S.E.: 2009, *Astrophys. J.*, **702**, 580.

Milano, L.J., Dmitruk, P., Mandrini, C.H., & Gómez, D.O.: 1999, *Astrophys. J.*, **521**, 889.

Moffatt, H.K.: 1985, *J. Fluid Mech.*, **159**, 359.

Moffatt, H.K.: 1986, *J. Fluid Mech.*, **166**, 359.

Moffatt, H.K., & Ricca, R.L.: 1992, Proc. R. Soc. Lond. A, **439**, 411.

Moffatt, H.K., Zaslavsky, G.M., Comte, P., & Tabor, M. eds.: 1991, *Topological Aspects of the Dynamics of Fluids and Plasmas*. NATO ASI series. Series E: Applied Sciences; Vol. 218. Kluwer Academic Publishers. ISBN 978-90-481-4187-6.

Nickerson, H.K., Spencer, D.C., & Steenrod, N.E.: 1959, *Advanced Calculus*, Van Nostrand, Princeton NJ. p. 95-97.

Parnell, C.E., Smith, J.M., Neukirch, T., & Priest, E.R.: 1996, *Phys. Plasmas*, **3**, 3.

Pontin, D.I., Galsgaard, K., Hornig, G., & Priest, E.R.: 2005, *Phys. Plasmas*, **12**, 052307.

Priest, E.R., & Démoulin, P.: 1995, *J. Geophys. Res.*, **100**, 23.443.

Priest, E.R., Heyvaerts, J.F., & Title, A.M.: 2002, *Astrophys. J.*, **576**, 533.

Priest, E.R., Longcope, D.W., & Heyvaerts, J.F.: 2005, *Astrophys. J.*, **624**, 1057.

Ricca, R.L. ed.: 2001, *An Introduction to the Geometry and Topology of Fluid Flows*. NATO Science Series. Series II. Mathematics, Physics and Chemistry; Vol. 47. Kluwer Academic Publishers. ISBN 978-1-4020-0207-6.

Ruzmaikin, A., & Akhmetiev, P.: 1994, *Phys. Plasmas*, **1**, 331.

Ruzmaikin, A., & Berger, M.: 1998, *Astron. Astrophys.*, **337**, L9.

Schindler, K., Hesse, M., & Birn, J.: 1988, *J. Geophys. Res.*, **93**, 5547.

Schmieder, B., Aulanier, G., & Vršnak, B.: 2015, *Solar Phys.*, **290**, 3457.

Scott, R.B., Pontin, D.L, & Hornig, G.: 2017, *Astrophys. J.*, **848**, 117.

Seehafer, N.: 1986, *Solar Phys.*, **105**, 223.

Somov, B.V.: 1992, *Physical processes in Solar Flares*. Astrophysics and Space Science Library (ASSL) series, vol. 172, Kluwer Academic Publishers. ISBN: 0-7923-1261-9

Syrovatskii, S.I.: 1981, *Astron. Astrophys. Rev.*, **19**, 163.

Tassev, S., & Sevcheva, A.: 2017, *Astrophys. J.*, **840**, 89.

Taylor, J. B.: 1986, *Rev. Mod. Phys.*, **58**, 3, 741.

Taylor, M. E.: 1996, *Partial Differential Equations Basic Theory*. Texts in Applied Mathematics 23, eds., Marsden, J. E., Sirovich, L., Golubitsky, M., & Jager, W., Springer-Verlag, New York.

Titov, V.S.: 1999, *Magnetic Fields and Solar Processes.* The 9th European Meeting on Solar Physics. 12-18 September, 1999. Florence, Italy. Ed. A. Wilson. European Space Agency, ESA SP-448. ISBN: 92-9092-792-5.

Titov, V.S.: 2007, *Astrophys. J.*, **660**, 863.

Titov, V.S., & Démoulin, P.: 1999, *Astron. Astrophys.*, **351**, 707.

Titov, V.S., Hornig, G., & Démoulin, P.: 2002, *J. Geophys. Res.*, **107**, 1164.

Titov, V.S., Priest, E.R., & Démoulin, P.: 1993, *Astron. Astrophys.*, **276**, 564.

Wang, Y.M., & Sheeley, N.R.: 1990, *Astrophys. J.***355**, 726.

Wolfson, R.: 1989, *Astrophys. J.*, **344**, 471.